

**CHARACTERIZATION OF BIOREACTORS AND SCALING DOWN OF
Escherichia coli CULTURE IN A VACCINE MANUFACTURING PROCESS**

Nathalia Andrea Carreño Medina

Chemical engineer

MASTER'S DEGREE IN CHEMICAL ENGINEERING

Director

Viviana Sánchez Torres

Chemical engineer, Ph.D.

Co-Director

Cecile Lemaitre

Mechanical and energy engineer, Ph.D.

Tutor

Mounir Zine

Biotechnological engineer

Universidad Industrial de Santander
Facultad de ingenierías Físicoquímicas
Escuela de Ingeniería Química
Bucaramanga

2024

ACKNOWLEDGMENTS

This research project is the result of a work involving the intervention of many people who contributed their knowledge in different fields to achieve a correct conduct of the experiments.

First of all, I would like to express my gratitude to the two people who gave me the opportunity to develop this internship project at Sanofi: Mrs. Faily, manager of the fermentation pilot unit and Mr. Zine, my internship supervisor.

A special thanks to my internship supervisor, Mr. Zine, who with his sympathy and good energy, always accompanied me in the development of the project. I would like to thank him for his willingness to teach me, to guide me, to answer my questions and to take me out of my comfort zone for the success of this project and of my professional career.

I would then like to thank Mrs. Palatin and Mr. Madi, senior technicians of the laboratory, who were kind enough to help me with all the preparations of the experiments and also to answer my questions. I would also like to thank Mr. Jeanne, who is part of the DataScience pole, for his collaboration and support in all the mathematical part developed around my internship.

I would also like to thank the entire MTech Sanofi team for their welcome, their recommendations and their company, which created a pleasant working environment.

Thank you to professor Viviana Sánchez from UIS, who was guiding and advising me throughout the entire process with the university. Also to professor Julio Pedraza and professor Cécile Lemaitre, who were attentive to the progress of the process with the UIS.

Finally, a big thank you to my mother and father, Erika and Marlon, for their advice and their unconditional support, both moral and economic part. I would also like to thank my brothers, Diego and Santiago, who believe in me and are my motivation to continue with my professional projects.

TABLE OF CONTENTS

1. PROBLEM STATEMENT 12

2. THEORETICAL FRAMEWORK..... 13

2.1. SANOFI13

2.2. SCALING UP OF BIOPROCESSES14

2.2.1. *OXYGEN VOLUMETRIC TRANSFER COEFFICIENT* 17

2.2.2. *CO₂ STRIPPING* 18

2.3. DIGITAL SCALING TOOL19

2.4. MENB VACCINE.....20

2.5. BACTERIA *ESCHERICHIA COLI*.....22

2.5.1. *THE STRAINS* 22

2.6. BACTERIAL CULTURE PROCESS23

2.7. DESIGN OF EXPERIMENTS.....24

3. OBJECTIVES 25

3.1. GENERAL OBJECTIVES25

3.2. SPECIFIC OBJECTIVES26

4. METHODOLOGY 26

4.1. CHARACTERIZATION OF BIOREACTORS26

4.1.1. *EXPERIMENTAL WORK*26

4.1.2. *BIOREACTORS*28

4.1.3. *DETERMINATION OF THE OXYGEN DENSITY TRANSFER COEFFICIENT*30

4.1.4. *PREDICTIVE MODELS OF THE OXYGEN VOLUME TRANSFER COEFFICIENT*31

4.2. EVALUATION OF THE MODELS ON THE *E. COLI* CULTURE PROCESS.....32

4.2.1. *E. COLI CULTURE PROCESS*32

4.2.2. *CASE OF STUDY: SCALE-DOWN OF THE MENB PROCESS*36

4.2.2.1. *SELECTION OF SCALE TRANSPOSITION CRITERIA*.....36

4.2.2.2. *SCALE TRANSPOSITION*.....37

4.2.2.3. *DETERMINATION OF OXYGEN VOLUMETRIC TRANSFER COEFFICIENT*.....38

4.2. *MODELS ADAPTATION*.....39

5. RESULTS AND DISCUSSION 40

5.1. CHARACTERIZATION OF BIOREACTORS40

5.1.1. *RESULTS OF THE OXYGEN VOLUME TRANSFER COEFFICIENT*.....40

5.1.2. *STATISTICAL ANALYSIS OF RESULTS*.....41

5.1.3. <i>PREDICTIVE MODELS</i>	44
5.2. MENB COLI CULTURE PROCESS	49
5.2.1. <i>CULTURE</i>	49
5.2.2. <i>BIOMASS PRODUCTION</i>	56
5.2.3. <i>ANTIGEN PRODUCTION</i>	56
5.2.4. <i>OXYGEN VOLUME TRANSFER COEFFICIENT</i>	58
5.2.5. <i>MODELS VALIDATION</i>	60
6. CONCLUSIONS AND PERSPECTIVES	63
BIBLIOGRAPHIC REFERENCES	62
APPENDIX	65
APPENDIX I	65
APPENDIX II	67
APPENDIX III	69
APPENDIX IV	70
APPENDIX V	72
APPENDIX VI	73
APPENDIX VII	75
APPENDIX VIII	76

TABLE OF FIGURES

Figure 1. Representation of scaling under modification [6]. 15

Figure 2. Process scaling methodology. 16

Figure 3. Representation of the mass transfer from the gas bubble to the cell. [9]. 17

Figure 4. Process of recombinant protein vaccine production. [19]. 21

Figure 5. Graphs obtained with the CCD method. (1) Points of the operating conditions. (2) Response surface. 25

Figure 6. Ambr250 bioreactor vessels. [30]. 28

Figure 7. Biostat bioreactor [31]. 29

Figure 8. Block diagram of the PID control. 35

Figure 9. Influence of agitation and aeration rate in $k_L a$. (1) Ambr250 (2) Biostat 43

Figure 10. Influence of agitation and aeration rate in UpH/min. (1) Ambr250 (2) Biostat. 44

Figure 11. Comparison of theoretical and experimental $k_L a$ results - Ambr250. 46

Figure 12. Comparison of theoretical and experimental $k_L a$ results - Biostat. 46

Figure 13. Comparison of statistical and experimental $k_L a$ results (1) Ambr250 (2) Biostat. 47

Figure 14. Comparison of statistical and experimental UpH/min results (1) Ambr250 (2) Biostat. 49

Figure 16. Recording of process monitoring parameters throughout the experiment in bioreactor 1 (Ambr250). 51

Figure 17. Recording of process monitoring parameters throughout the experiment in bioreactor 3 (Ambr250). 52

Figure 18. Recording of process monitoring parameters throughout the experiment in bioreactor 7 (Ambr250). 52

Figure 19. Recording of the process monitoring during culture of the Biostat experiment. 53

Figure 20. Evolution of pO_2 throughout the Biostat experiment. 54

Figure 21. Comparison of stirring condition profiles between the Biostat and the 5L reference bioreactor. 55

Figure 22. Comparison of O_2 flow condition profiles between the Biostat and the 5L reference bioreactor. 55

Figure 23. Cellular growth kinetics. 56

Figure 24. Protein concentration profile. 57

Figure 25. Results of the average of experimental and theoretical $k_L a$ - Ambr250..... 59

Figure 26. Comparison of modified $k_L a$ models in bio 3 (Ambr250). 60

Figure 27. $k_L a$ as a function of time in bio 3 (Ambr250). 61

Figure 28. Comparison of modified $k_L a$ models in Biostat. 62

Figure 29. $k_L a$ as a function of time in the Biostat. 62

Figure 30. Recombinant protein process. 68

Figure 31. Response surface of k_{La} - Ambr250. (1) As a function of conditions. (2) As a function of the parameters (P/V and U_g)..... 75

Figure 32. Response surface of the k_{La} - Biostat. (1) As a function of conditions. (2) As a function of the parameters (P/V and U_g)..... 75

Figure 33. Profile of the 5 L bioreactor. (1) Operating conditions. (2) pO_2 regulation. 77

Figure 34. Results from the 5 L bioreactor. (1) Cell growth. (2) Antigen concentration. 77

TABLE OF TABLES

Table 1. Examples of E. coli strains [25]..... 22

Table 2. Parameters established for scaling down on the Ambr250 bioreactor..... 37

Table 3. Dependent and independent variables for linearization..... 40

Table 4. Results of kLa in the Ambr250 and Biostat bioreactors 40

Table 5. Influence of operating conditions and their interactions in kL a - Ambr250. 41

Table 6. Influence of operating conditions and their interactions in the kLa - Biostat. 43

Table 7. Influence of operating conditions and their interactions in UpH/min - Ambr250
..... 43

Table 8. Influence of operating conditions and their interactions in the UpH/min -
Biostat..... 44

Table 9. Coefficients of the theoretical correlation of kLa..... 45

Table 10. Coefficients of the statistical correlation of kLa..... 47

Table 11. Coefficients of the statistical correlation of UpH/min..... 48

LIST OF SYMBOLS AND ABBREVIATIONS
Nomenclature

a	Interfacial area (m^2/m^3)
X	Biomass
k_L	Transfer coefficient (m/s)
$k_L a$	Oxygen volumetric transfer coefficient ($1/\text{s}$)
$C_{O_2}^*$	Oxygen saturation (mol/m^3)
C_{O_2}	Oxygen concentration in the environment (mol/m^3)
$C_{O_2_0}$	Initial oxygen concentration in the medium (mol/m^3)
C_X	Biomass concentration (mol/m^3)
Q_g	Flow aeration (m^3/s)
DO	Optical density or dissolved oxygen
d	Dilution factor
pO_2	Partial pressure of oxygen (%)
P/V	Volumetric power input (W/m^3)
q_{O_2}	Specific oxygen level of the microorganism used ($1/\text{s}$)
N	Stirring speed (<i>rpm</i>)
U_g	Linear gas velocity (m/s)
r_{O_2}'''	Volume rate of O_2 ($\text{mol}/\text{m}^3\text{s}$)
vvm	Volume of air per volume of medium per minute ($1/\text{min}$)

Abbreviations

DNA	Deoxyribonucleic acid
RNA	Ribonucleic acid
BBD	BoxBehnken Design method
GMP	Good manufacturing practices
CCD	Central composite design method
CCRD	Central composite rotatable design method
DSP	Downstream processing
FCCF	Central face composite design method
HPLC	High Performance Liquid Chromatography.
IPTG	Isopropyl β -D-thiogalactopyranoside
OTR	Oxygen Transfer Rate
OUR	Oxygen Uptake Rate
DoE	Design of experiments
PID	Proportional - integral - derivative controller
RSM	Response surface methodology
USP	Upstream processing

ABSTRACT**Characterization of bioreactors and scaling down of *Escherichia coli* culture in a vaccine manufacturing process ***

Nathalia Andrea Carreño Medina**

Key words: $k_L a$, CO_2 stripping, Scale-down, *E. coli*, Modeling.**Abstract**

Scale up and scale down of vaccine manufacturing processes is one of the most studied challenges today. Most of these processes are aerobic, the oxygen volumetric mass transfer coefficient ($k_L a$), and the carbon dioxide stripping (CO_2 stripping) prove to be key levers for the characterization of bioreactors. This project proposes the study of these parameters for their application in the scale-down of the *Escherichia coli* culture in the production process of meningitis vaccine. Experimental work, at different agitation speeds and air flow rates, are carried out in a pilot fermentation unit where 250 mL and 2 L bioreactors were used. Subsequently, the scale transposition was performed using a digital tool to determine the control parameters to be applied on the 5 L bioreactor as reference scale. Among the observations, a high oxygen transfer and CO_2 stripping is achieved in the smallest bioreactor. In addition, the predictive power of the models and the transposition capacity of the tool have been demonstrated. Finally, a specific factor was determined to increase the performance of the models.

* Master Degree Work

** Faculty of Physicochemical Engineering. School of Chemical Engineering. Director: Viviana Sánchez Torres. Chemical engineer, Ph.D. Co-Director: Cecile Lemaitre. Mechanical and energy engineer, Ph.D. Tutor: Mounir Zine. Biotechnological engineer

RESUMEN**Characterization of bioreactors and scaling down of *Escherichia coli* culture in a vaccine manufacturing process ***

Nathalia Andrea Carreño Medina**

*Palabras clave: k_La , Extracción de CO₂, escalado, E. coli, Modelamiento.***Descripción**

La transposición de pequeña a grande escala y de grande a pequeña escala de los procesos de fabricación de vacunas es uno de los desafíos más estudiados en la actualidad. La mayoría de estos procesos son aeróbicos, por ende, el coeficiente de transferencia volumétrica de masa de oxígeno (k_La) y la extracción del dióxido de carbono (Extracción del CO₂), resultan ser parámetros clave para la caracterización de biorreactores. Este proyecto propone el estudio de estos parámetros para su aplicación en el escalado del cultivo de *Escherichia coli* en el proceso de producción de la vacuna contra meningitis. Se realizaron trabajos experimentales, a diferentes velocidades de agitación y caudales de aire, en una unidad piloto de fermentación donde se utilizaron biorreactores de 250 mL y 2 L. Posteriormente, se realizó la transposición de escala mediante una herramienta digital para determinar los parámetros de control a aplicar en el biorreactor de referencia, el cual tiene un volumen de 5 L. Entre las observaciones, se logra una alta transferencia de oxígeno y extracción de CO₂ en el biorreactor más pequeño. Además, se logró demostrar el poder predictivo de los modelos y la capacidad de transposición de la herramienta. Finalmente, se determinó un factor específico para incrementar el rendimiento de los modelos.

* Trabajo de Grado de Maestría

** Facultad de Ingenierías Físicoquímicas. Escuela de Ingeniería Química. Directora: Viviana Sánchez Torres. Ingeniera Química, Ph.D. Co-Director: Cecile Lemaitre. Ingeniera Mecánica y de Energía, Ph.D. Tutor: Mounir Zine. Ingeniero Bioquímico.

1. PROBLEM STATEMENT

An internship was carried out on the Sanofi Marcy l'Etoile site, where research and production of vaccines are at the heart of the site. Vaccines contain several components that guarantee their efficacy and safety [1]. For this reason, the production process is divided into different stages and must comply with Good Manufacturing Practices (GMP). During the vaccine manufacturing process, the first step (upstream) is the production of the antigen in the bacterial or viral culture. The second step (downstream) is purification, which aims to extract and purify the antigen from the culture.

One of the challenges facing the pharmaceutical industry today is the scaling-up/scaling-down of processes. Currently, scaling-up is achieved largely using process engineering and biotechnology principles. The principles of scaling-up studies are based on the knowledge of the interaction between the mass transfer, the heat transfer, and the biological part of the system. This internship was focused on gas-liquid mass transfer, especially the mass transfer coefficient ($k_L a$) and CO₂ stripping.

To control the specific parameters for each scale, it is important to establish descriptive models of the bioreactors. Characterization can be done in the absence of microorganisms to facilitate experiments and reduce costs. However, the evaluation of these models in cell culture processes is key to validate their predictive power. For this reason, the *Escherichia coli* culture process for the manufacture of the MenB vaccine is the focus of this project. Since this process is in the development/industrialization phase, the evaluation of the culture parameters applied at different scales is essential.

In this context, it is important to have descriptive models for bioreactors of different scales to be able to make a good prediction of material transfer. First, we will discuss the methods used to characterize bioreactors. We will then present the

computational tool developed for scaling whose predictive power will be evaluated on the *E. coli* culture process. Finally, we will analyze the results obtained and evaluate the accuracy levels of the models established to characterize the descriptive variables studied.

2. THEORETICAL FRAMEWORK

2.1. Sanofi

Sanofi is a French pharmaceutical company dedicated to the innovation of treatments and vaccines since 1973. The company produces a wide range of healthcare products, such as vaccines, drugs, and medical devices.

In the healthcare sector, Sanofi ranks third worldwide in terms of sales. Sanofi is present in more than 100 countries around the world and has 112 industrial sites in 40 countries. Thanks to its strong presence, the company employs more than 100,000 people. Sanofi is divided into several entities:

- Sanofi Pasteur: specialized in vaccines.
- Sanofi Genzyme: specialized in biotechnologies.
- Sanofi R&D: specialized in research and development.
- Sanofi Chimie: specialized in chemical and biotechnological production.
- Sanofi Aventis: specialized in generic drugs.

The site where this internship took place is located in Marcy l'Etoile, near Lyon. This site is one of the largest Sanofi sites in the world. It is dedicated to Sanofi's vaccine activity and includes the R&D, industrialization and production departments. It is also the largest R&D center in the vaccines business and a center of excellence for new vaccine projects.

The internship took place in the pilot fermentation platform of the bacteriology area, which is dedicated to the optimization of bacterial vaccine processes, industrialization, and production support.

2.2. Scaling up of bioprocesses

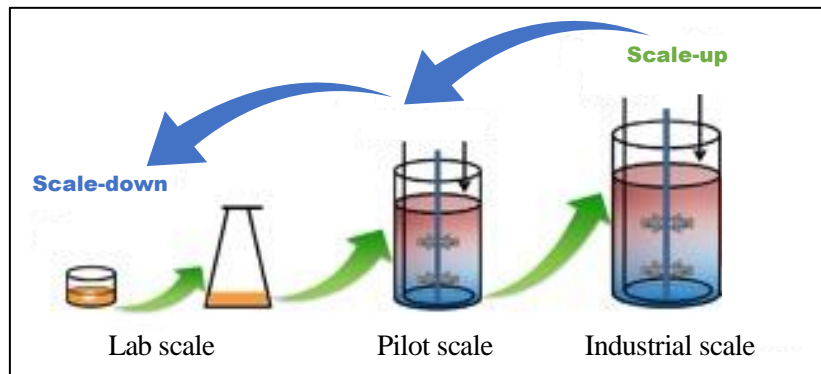
The development of a bioprocess starts on a small scale to define the optimal culture conditions and parameters. However, these parameters cannot be directly applied on a large scale [2]. For this reason, it is necessary to find a suitable methodology to transpose a cell culture process from one scale to another to ensure a comparable microenvironment for the cells regardless of the bioreactor size.

The understanding of fluid mechanics serves as a basis for establishing a consistent microenvironment for cells [3]. In this sense, it is important to study not only the physiological state of the cells but also the hydrodynamics of the system [4]. Indeed, the hydrodynamics of the material transfer influences both the convective and the diffusive transport of the system.

As far as scaling is concerned, it can be done not only from small to large scale (Scale-up), but also from large to small scale (Scale-down). This last transposition aims at analyzing and finding solutions for anomalies that are present on a large scale, even on an industrial scale. The goal is to reproduce a process on a small scale by considering the constraints encountered on an industrial scale [5]. Once the scaling is achieved and a representative model is available, the analysis of solutions to the problems can begin. A schematic representation is presented in **Figure 1**.

Figure 1.

Representation of scaling under modification [6].

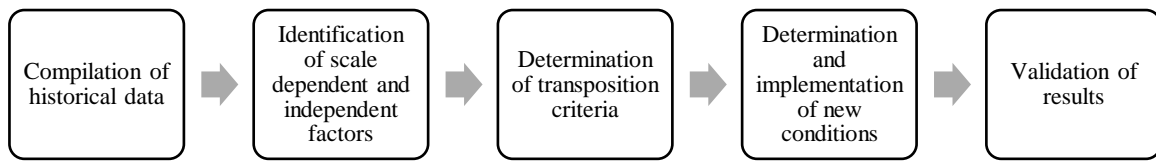


Chemical engineering and bioprocess engineering aspects are the basis for classical methodologies of process scaling [7]. Process scaling starts with the analysis of the bioprocess parameters at a reference scale, and then these parameters were adapted to the target scale. These parameters are established based on factors that describe the bioreactor that could be scale-dependent or scale-independent [5]. The determination of the scale-dependent factors is done both by linear interpolation (volumes) and by theoretical equations (stirring speed and aeration rate). In addition to these, there are scale-independent factors, such as temperature, medium, pH, and culture time.

Once the factors have been identified, the transposition methodology begins. This methodology is based on transposition criteria that are kept constant during the scaling process. The transposition criteria used in practice at the industrial level are volumetric power input, oxygen volume transfer coefficient, tip velocity, and dissolved oxygen concentration [7]. **Figure 2** shows a representative schematic of the methodology applied to this scaling study.

Figure 2.

Process scaling methodology.



It has been shown that scaling up consists in following the evolution of the bioreactor operating parameters.

In general, agitation and aeration play a fundamental role in the mass transfer. Indeed, mixing, shear stress, oxygen transfer, and CO₂ stripping are strongly influenced by these conditions. In most cases, the ratio of air volume per volume of medium per minute (*vvm*) is chosen as the scaling criterion, so aeration acts proportionally as a function of scale. For this reason, it is important to pay attention to foam generation, as deep aeration generates an increase in foam in the bioreactor, which can lead to clogging of the gas outlets.

Oxygen supply and removal of dissolved carbon dioxide are among the most important factors in mass transfer. In addition, aerobic processes use cells that require oxygen for their development because it is the final electron acceptor in the cellular respiration chain [8]. Regarding CO₂, it is produced by the cells during the respiration process. Nevertheless, a high concentration of dissolved CO₂ could negatively impact cell growth and antigenic productivity in some bioprocesses.

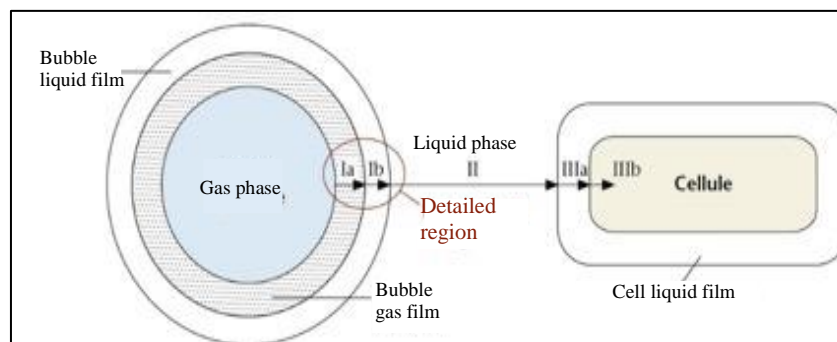
E. coli culture is carried out in stirred bioreactors. This equipment is characterized by specific parameters, such as material, size, type of agitation, among others. It is in this context that the need arises to characterize bioreactors of different scales to improve the mastery and the representativeness of the scale-down and scale-up of the same process.

2.2.1. Oxygen volumetric transfer coefficient

Mass transfer occurs when a gas is introduced into the bioreactor to meet the needs of the microorganisms. The system then becomes a gas-liquid system under mechanical agitation. A graphical representation is presented in **Figure 3**, where the **detailed region** refers to the determining step. This material transfer corresponds to the transfer of the gaseous oxygen contained in the gas bubble, to the liquid phase which is the culture medium [3].

Figure 3.

Representation of the mass transfer from the gas bubble to the cell [9].



The oxygen transfer step is described by the transfer coefficient and the oxygen concentration gradient [3]. It is important to emphasize that the transfer coefficient concerning the gas phase is negligible due to the low viscosity and high diffusivity of gases. Moreover, the coefficient that describes this type of process is often the volume transfer coefficient ($k_L a$). This coefficient is calculated with the transfer coefficient (k_L), which depends on the hydrodynamics and properties of the liquid, and the interfacial area (a) which depends on the amount of gas retained and the size of the bubbles present in the bioreactor [3].

In this sense, the system has a supply of oxygen through aeration using air or pure oxygen, as well as consumption by the cells. These are characteristic factors of an aerobic bioprocess, which are defined by the OTR (Oxygen Transfer Rate) and the OUR (Oxygen Uptake Rate). The mass balance concerning the quantity of oxygen in a bioreactor is:

$$\frac{dC_{O_2}}{dt} = OTR - OUR \quad (1)$$

$$\frac{dC_{O_2}}{dt} = k_L a (C_{O_2}^* - C_{O_2}) - r_{O_2}'' \quad (2)$$

$$\frac{dC_{O_2}}{dt} = k_L a (C_{O_2}^* - C_{O_2}) - q_{O_2} C_X \quad (3)$$

Where, $C_{O_2}^*$: oxygen saturation.

C_{O_2} : oxygen concentration in the liquid phase.

q_{O_2} : specific oxygen level of the microorganism used.

C_X : Biomass concentration.

As presented in equation $\frac{dC_{O_2}}{dt} = k_L a (C_{O_2}^* - C_{O_2}) -$

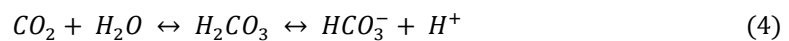
$q_{O_2} C_X$ (3), the mass balance allows us to model the oxygen

volumetric transfer coefficient. It is therefore necessary to determine the value of $k_L a$.

The most common methods applied in a microbial bioprocess can be classified according to whether the measurement is performed in the absence of microorganisms, using dead cells, or in the presence of biomass that consumes oxygen at the time of measurement [10].

2.2.2. CO₂ stripping

Carbon dioxide plays an important role in bioprocess. Cells need it because it helps to mimic in vivo conditions through pH control. Thus, many processes use the injection of CO₂ for its efficiency in acidic pH regulation. The equation (4) describes the chemical reaction that is set up during the presence of CO₂.



Although the presence of CO₂ is important, its removal is required because it can negatively impact the performance of the bioprocess in case of high concentration. In the case of bacterial culture processes, the injection of gas (air, oxygen, or nitrogen) contributes to the stripping of CO₂ (CO₂ removal) [11]. This is a technique used to remove

toxic gases during fermentation [12]. However, the size of the bubbles becomes an important parameter because if they are too small, the CO₂ passes back into the liquid before reaching the surface, preventing the removal of CO₂.

An important parameter related to CO₂ stripping performance is the size of the bioreactor. Indeed, the larger the bioreactor, the more CO₂ accumulates, and the lower the CO₂ stripping capacity. As a rule, the best performances are present in small-scale bioreactors due to the increase of the sprinkler rate [11].

2.3. Digital scaling tool

The Mtech department has bioreactors of different sizes for all the studies and projects that are carried out there. The role of the pilot fermentation unit is to develop industrial processes, improve already industrialized processes, or help the production area by solving anomalies or deviations of commercial products. In this context, the same process is worked on at different scales, from the small laboratory bioreactor of 250 milliliters to the industrial bioreactor of 1000 liters. To answer the numerous questions that scale-up or scale-down of bacterial culture processes raises, the pilot unit has initiated the design of a digital tool supported by a methodology that facilitates both the calculations and the prediction of the hydrodynamic environments present inside each bioreactor according to the applied regulation parameters.

The development of this tool began in 2020 and was conducted in three stages:

- First, the compilation of all the parameters that are involved in a bioprocess, as well as their respective formulas. In these calculations, the $k_L a$ is also included. However, this tool used a general model (*Van't Riet equation*) for all sizes of bioreactors, which is described in the *Bioreactors section*.
- In February 2022, the second part of the project started. The objective of this step was to feed the tool with specific models for each of the scales for the $k_L a$ and

CO₂ stripping. Thanks to this work, the tool now has specific predictive models for each bioreactor present in the fermentation pilot lab [13]. This characterization of the bioreactors was done in the absence of microorganisms.

- In January 2023, the third step of the project started. This step is the application of these models in a process in bacterial culture, to evaluate the predictive power of the models as well as the capacity of transposition of the scales.

All bioreactors in the bacteriology area are registered in the scaling tool. This required initially the compilation of the geometrical data of each fermenter using the documents given by the suppliers. From these data, other descriptive variables are calculated to characterize the hydrodynamic constraints present inside each bioreactor (e.g., Reynolds number, volumetric power input, etc.).

Once the bioreactors have been selected, the theoretical scaling study is carried out by applying different values to the process control parameters (agitation, aeration, etc.). The objective is to keep constant the critical parameters for the process and to accept to let vary those which are less critical. In this way, the tool allows the selection of the operating set points which will be interesting to evaluate in the laboratory. Moreover, two graphs have been developed on this interface to facilitate the visual interpretation of the results in the form of a dashboard. *APPENDIX I* shows a screenshot of the tool developed.

2.4. MenB Vaccine

Meningitis is an infectious disease that affects the cerebrospinal fluid (the fluid that flows between the meninges) by causing inflammation of the membrane that surrounds the central nervous system [14]. This disease is caused by a virus or a bacterium. Bacterial meningitis is less common but more serious because it can affect the central nervous system or even the entire body. This type of meningitis is triggered by

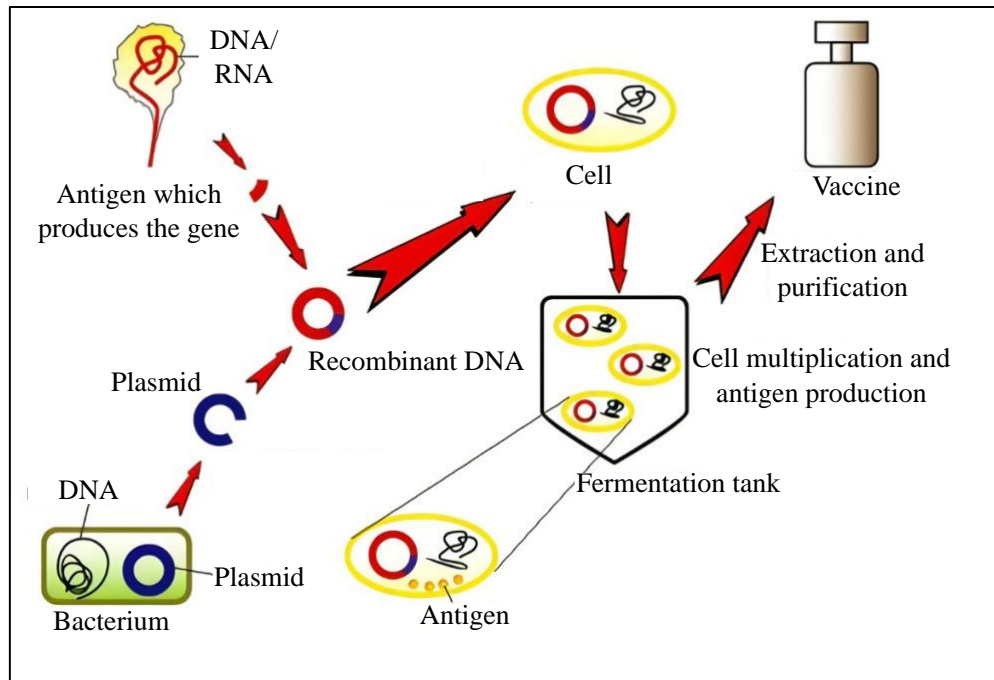
various bacteria, such as *Pneumococcus*, *Meningococcus*, *Listeria*, or *Haemophilus influenzae* [15].

The bacterium most likely to cause a major epidemic is *Neisseria meningitidis* [16]. There are several serogroups of this bacterium, of which the following six are known to cause epidemics: A, B, C, W135, X, and Y [17]. For this reason, it has become necessary to develop a vaccine to combat the disease.

The meningococcal type B vaccine is currently under development at Sanofi. It is a recombinant vaccine, meaning that the antigen it contains is a recombinant protein. The production of this protein results from the expression of a gene integrated into a plasmid by a host cell after the transformation of the latter [18]. The production of the recombinant protein is often subject to induction by the addition of substrate, temperature change, or nutrient deprivation. In this case, the expression must be induced by the addition of IPTG (Isopropyl β -D-thiogalactopyranoside). The process of induction is described in APPENDIX II. A general representation of this process is shown in **Figure 4**.

Figure 4.

Process of recombinant protein vaccine production [19].



2.5. Bacteria *Escherichia coli*

The *E. coli* bacterium is used as a host to produce recombinant proteins for various biotechnological applications due to its many advantages, such as its ease of cultivation in the laboratory due to [20] :

- Minimum and simple nutritional requirements,
- A very short doubling time (20 minutes).
- An ability to survive for several days and grow outside a host.

E. coli is a bacterium with a Bacillus-like morphology, which is rod-shaped [21]. It is a Gram-negative facultative aerobic and anaerobic bacterium, which means that it can grow both in the presence of oxygen (aerobic atmosphere) and in the absence of oxygen (anaerobic atmosphere).

Regarding its biochemical characteristics, *E. coli* can use glycerol, glucose, acetate, mannitol, and lactose as a carbon source [22]. *E. coli* grows between 15 °C and 45 °C and has optimal growth at 37 °C [16]. Regarding the optimal culture pH, this bacterium tolerates pH values between 6 and 8 with an optimal growth pH of 7.

Among other characteristics of *E. coli*, the low secretion potential is representative, as well as the low or no post-translational modifications [23]. This is the reason why this bacterium is used in various industrial applications. Nevertheless, the absence of post-translational modifications is also the reason why this bacterium cannot be used to produce too complex human or animal proteins.

2.5.1. The strains

A strain is a genetic variant or subtype of a microorganism or virus [24]. Some *E. coli* strains used as expression vectors are presented in **Table 1**:

Table 1. Examples of E. coli strains [25].

Strain	Features
BL21	Expression without T7 system
BL21(DE3)	Expression T7
NEB Express	Versatile expression strain without T7 system
SHuffle T7	Strain K12 for expression T7 Correct folding of disulfide-bridged proteins in the cytoplasm

The two strains most used commercially to produce recombinant proteins are BL-21 and K-12 (SHuffle T7). The selection is based on three reasons. First, this strain has high protein stability due to the absence of protease enzymes. In addition, acetate production is low, so growth inhibition is also low. Finally, it is a strain with high membrane permeability.

2.6. Bacterial culture process

Vaccine production processes always follow the same protocol. In these processes, there are two main parts: Upstream process (USP) and Downstream process (DSP). The USP is the first part of the process and corresponds to the production of the molecule of interest in a bioreactor. Once the molecule is produced, the second part (DSP) starts. The DSP will then isolate and purify the molecule to prepare it for the following

steps: formulation, control, and packaging. However, during this project, the focus is on the USP part.

The bacterial amplification or industrial culture is a phase of the process that takes place in a bioreactor. This step consists in amplifying the quantity of bacterial cells to activate the production of recombinant proteins. It is important to specify that a preculture step is required before starting this phase.

During bacterial amplification, it is essential that the culture conditions are optimal to produce maximum biomass in minimum time. The key parameters of this amplification process are temperature, pH, oxygen, system agitation, and medium. It is therefore necessary to control these parameters.

2.7. Design of experiments

The response surface method (RSM) is a mathematical and statistical technique that assists in the analysis of experimental results, as well as the construction of an empirical model that assists in the prediction of results in the laboratory [26]. This method also helps to find the conditions to be evaluated in the experiments to be done in the laboratory, covering a wide range of values of the operating variables [27]. For the design of experiments, it is strongly used because it allows the evaluation of different factors and their interactions.

In order to plan the experimental design, the Central Composite Design (CCD) method was selected. It consists of three parts: a factorial design, a center point, and the points on the axis of each factor [28]. In this way, the model will be of the second degree, in the form:

$$Y = a_o + \sum a_i x_i + \sum a_{ij} x_i x_j + \sum a_i x_i^2 \quad (5)$$

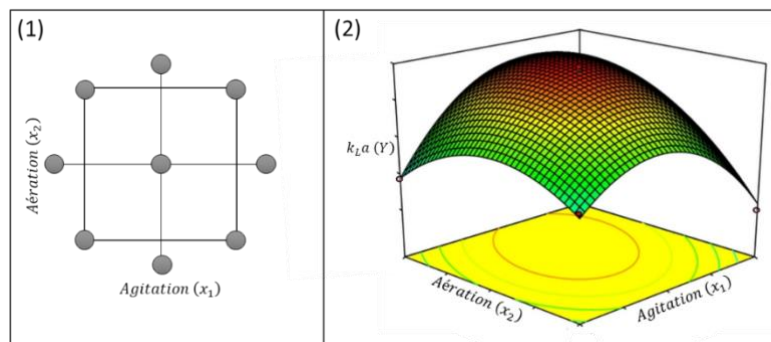
In this method, coded variables are considered. At the end of the experimental work, there will be a final equation that will predict future results in the laboratory. This

equation will be a function of the coefficients found and their interactions. It is important to highlight that the two response variables of this project are: the $k_L a$ and the CO₂ stripping. Indeed, a descriptive equation will be found for each of the two variables.

Based on the theory presented earlier, the two variables to be used for bioreactor characterization were the bioreactor stirring speed (x_1) and the air flow rate (x_2). For this reason, to have a good coverage of the conditions in each bioreactor, it was necessary to know the minimum and maximum values specific to each equipment. Thus, the method allows to obtain a wide spectrum of operating conditions to be set up and a response surface, as presented in *Figure 5*.

Figure 5.

Graphs obtained with the CCD method. (1) Points of the operating conditions. (2) Response surface.



In general, specific and detailed information is required for each bioreactor, where in addition to their information on dimension and geometry values, the minimum and maximum operating conditions are also needed. After this, it is important to establish the operating ranges based on the conditions that are implemented in the laboratory tests. Finally, these values are taken into account for the DoE, where 4 central points are included in order to evaluate repeatability. This conditions are presented in the section 4.1.2.

3. OBJECTIVES

3.1. General objectives

Characterize the volumetric coefficient of mass transfer, and CO₂ stripping of two bioreactors of different sizes, 250 mL and 2 L, from the pilot fermentation laboratory to improve the scale transposition tool and have descriptive models for each type of bioreactor.

3.2. Specific objectives

- 1) Define the specific models of the volumetric mass transfer coefficient, and the CO₂ stripping for both the 250 mL bioreactor and the 2 L bioreactor.
- 2) Determine the new process conditions for the scale-down of the *MenB coli* vaccine manufacturing process.
- 3) Assess the predictive power of the scaling tool and its models.

4. METHODOLOGY

4.1. Characterization of bioreactors

As presented in *the Scaling up of bioprocesses section (2.2)*, after the compilation of all the parameters and formulas that are involved in a bioprocess, the characterization of the bioreactors by defining predictive models specific to each scale takes place. These models allow the prediction of the quality of gas exchange for each of the scales studied thanks to 2 descriptive variables (the $k_L a$ and CO₂ stripping). This characterization was performed for 88% of the equipment during my first internship in 2022. This master's thesis corresponds to the remaining 12% which are presented in *Bioreactors section*.

4.1.1. *Experimental work*

In a bioreactor characterization study, it is recommended to work without microorganisms to facilitate the experiments and reduce costs. Also, the evaluation of the data is easier and can be done very quickly and it was necessary to work under sterile conditions [29]. In addition, the characterization can cover a wide range of condition values because there were no restrictions on the side of the biological system.

For the experiments that are carried out in the laboratory, a sodium bicarbonate buffer solution (NaHCO_3) has been developed. The interest of using this buffer solution was to be able to follow the evolution of the dissolved O_2 and the pH at the same time. Indeed, the evolution of the pH of the sodium bicarbonate solution being proportional to the elimination of dissolved CO_2 , this technique allows to follow at the same time the transfer of O_2 in the medium and the CO_2 stripping.

Two probes were used throughout the experiments: the electrochemical probe pO_2 and the pH probe. Before starting the experiments, these probes must be calibrated. The pH probe is calibrated with 2 buffer solutions of pH 7 and pH 10, then it is installed in the bioreactor. For the PO_2 probe, the 100% calibration is performed in air, then the probe is placed in a nitrogen saturated atmosphere to verify that the time taken by the probe to go from 100% to <5% O_2 is less than 1 min. The pO_2 probe is then installed in the fermenter.

The temperature control is then started with a set point of 37 °C and a stirring speed sufficient to ensure the homogeneity of the tank. Once the set point temperature is reached, the pH and pO_2 sensors are checked:

- pH probe: a sample of the buffer contained in the bioreactor is taken to verify on a benchtop pH meter that the pH read by the fermenter probe is accurate.
- pO_2 probe: a new calibration of the 100% is performed at maximum agitation and aeration conditions of the bioreactor.

For the gas transfer study, the system must be at low pO_2 and pH 7. For this reason, a deep injection of nitrogen is performed to remove dissolved oxygen. Once the oxygen is completely removed ($pO_2 < 5\%$), it is necessary to lower the pH by injecting CO_2 . Once the conditions presented previously are met, the experiments start following the design of experiments (DoE) that were found for each bioreactor. A specific DoE was designed for each bioreactor (section 4.1.2), and it is based on the minimal and maximal conditions.

The DoE implementation is based on changing the conditions of aeration flow and agitation speed. Therefore, the handling of the gas supply valves, as well as the control of the agitation, is essential. It is important to note that the nitrogen flow rate is used to lower the amount of dissolved O_2 and the CO_2 flow rate to control the pH to 7.

4.1.2. Bioreactors

The pilot fermentation team has several types of bioreactors. Within these bioreactors are stainless steel and single-use bioreactors. These are bioreactors of different sizes, where the Ambr250 bioreactor and the Biostat bioreactor are the case of study for the development of this master's project [13].

4.1.2.1. Ambr250

The Ambr250 Bioreactor (Sartorius, France) operates on an automated system of 12 single-use 250 mL bioreactors. Although it is an automated system, each bioreactor operates independently of the others through an individual control system [30]. The Ambr250 has two types of vessels to cover a wide range of experiment types.

The case of study of this project is the microbial tanks. These tanks are composed of mobile Rushton turbine type stirrers. Each control unit of each bioreactor is equipped with liquid and gas supply connectors, a single-use pH electrode, a measuring tablet pO_2 (DO), a heating/cooling belt and a stirring motor. The bioreactors are shown in **Figure 6** [30].

Figure 6.

Ambr250 bioreactor vessels. [30].



As previously mentioned, it is necessary to know the minimum and maximum aeration and agitation capacities of the bioreactors, as well as the limited process conditions. For the Ambr250 Microbial these values are 150 to 4500 rpm for stirring speed, and $550 \text{ mL}/\text{min}$ for the maximum air sparger flow rate.

4.1.2.2. Biostat

The Biostat bioreactor (Sartorius, France) is a 2 L autoclavable borosilicate glass culture vessel (**Figure 7**) [31]. This bioreactor has the particularity of having different parts that allow the creation of different configurations for experiments in the laboratory. In addition, it has quick-connect fittings that facilitate the connection of all cables and supplies to the culture vessels [32]. Regarding the agitation parameter, it has Rushton agitation mobiles dedicated to microbial cultures and pitch-blade dedicated mainly to Eukaryotic cell cultures.

Figure 7.

Biostat bioreactor [31].



The range of stirring speeds is 20 to 2000 rpm and the maximum value of air sparger flow rate is 3 lpm. However, the characterization was based on the limits of the conditions of the experiments performed in the laboratory. These values are 20 – 1000 rpm for the stirring speed, and 0,2 – 3 lpm for the air flow rate. As for the Ambr250 system, the focus of this project is on the tanks dedicated to microbial cultures (Rushton agitation type).

4.1.3. *Determination of the oxygen density transfer coefficient*

4.1.3.1. Experimental method

The experimental determination is based on a descriptive expression of the oxygen concentration as a function of time. For this reason, it is necessary to start from *equation (3)* which was obtained from the bioreactor mass balance. However, the term OUR is removed from this expression due to the absence of microorganisms in the system. The descriptive equation will therefore be *equation (6)*.

$$\frac{dC_{O_2}}{dt} = k_L a (C_{O_2}^* - C_{O_2}) \quad (6)$$

In order to facilitate the calculation of $k_L a$ a numerical integration is made to have an expression of type $Y = mx + b$. This procedure is presented below.

$$\int_{C_{O_2o}}^{C_{O_2}} \frac{1}{(C_{O_2}^* - C_{O_2})} dC_{O_2} = \int_{t_o}^t k_L a dt \quad (7)$$

$$\text{Ln} \left(\frac{C_{O_2}^* - C_{O_2o}}{C_{O_2}^* - C_{O_2}} \right) = k_L a (t - t_o) \quad (8)$$

In this way, it is necessary to make a graph of $\text{Ln} \left(\frac{c_{O_2}^*}{c_{O_2}^* - c_{O_2}} \right)$ as a function of time to get the value of $k_L a$. This value corresponds to the slope of the graph.

4.1.3.2. Theoretical method

The theoretical determination is based on a descriptive expression found in the literature (*equation (9)*). This equation is proposed by Van't Riet and depends on the volumetric power input (P/V) and the linear gas velocity (U_g) [33]. For this reason, it is considered as the starting point for the characterization of bioreactors. It is a model that is a function of two parameters that are strongly influenced by agitation and aeration.

$$k_L a = 0,002 \cdot (P/V)^{0,7} \cdot (U_g)^{0,2} \quad (9)$$

It is important to note that this extracted equation is described in the literature for a given type of bioreactor. However, it is used as a base formula for all the bioreactors in the fermentation laboratory. In this sense, the first step of the scale characterization work is to define a similar equation for each bioreactor of the fermentation laboratory. To do this, it is necessary to calculate for each bioreactor the three coefficients (K, a, b) that are involved in the correlation (*equation (10)*). Its estimation was done by following and analyzing the results that were obtained during the experiments of $k_L a$.

$$k_L a = K \cdot (P/V)^a \cdot (U_g)^b \quad (10)$$

The methodology that was implemented for the determination of the coefficients K, a, b , is based on a linearization of *equation (10)* and then doing a multiple linear regression. For this graphical analysis, the calculations of the volumetric power input and the linear gas velocity was necessary. These parameters could calculate following the equations in APPENDIX IV. Once the coefficients were established, the estimation of $k_L a$ is done from the model found for each bioreactor.

4.1.4. Predictive models of the oxygen volume transfer coefficient

As mentioned earlier, this study use two predictive models of $k_L a$. Both models were used in the experimental results (section 4.1.1). However, the difference is that one model is a function of the agitation variables and air flow, while the other one is a function of the parameters of volumetric power input and linear gas velocity.

Obtaining these two models allows the comparison of the prediction potential of each equation. In addition, a three-dimensional response surface plot was made using Matlab (MathWorks, U.S) and JMP (JMP headquarters, U.S) applications to obtain a profile of the coefficients as a function of the conditions. However, it is important to note that these models are designed in the absence of microorganisms. For this reason, the application of the equations in a microbial process is crucial for the validation of the model and the analysis of the impact of the environment on the $k_L a$.

4.2. Evaluation of the models on the *E. coli* culture process

The second part of this study consists in the validation of the models found during the tests without microorganism. This validation is done through a bacterial bioprocess. It is the MenB coli vaccine process, which is in the industrialization phase at Sanofi. First, it was necessary to understand the functioning of the culture in order to intervene in the bioprocess to apply the material transfer models. After that, a scale transposition process took place to evaluate the predictive potential of the tool. Finally, an evaluation of the models was implemented by processing the results obtained. These results allowed to check if a model's adaptation is necessary to optimize the models in a microbial application.

4.2.1. *E. coli* culture process

4.2.1.1. Culture media and conditions

The medium used for cell multiplication and growth of *E. coli* is a chemically defined medium, where glucose is the main carbon source. The laboratory has the basic *MenB coli* medium for preculture and culture of the system. In addition, it is important to add trace elements (hydrogen diammonium phosphate, magnesium sulfate and monopotassium phosphate) that complete the medium.

The conditioning of the environment is done through the pH and foam control. For this reason, the provision of 5N ammonia and polypropylene glycol PPG P2000 are important. In addition, induction is done manually with an IPTG solution.

4.2.1.2. Bacterial amplification of the MenB vaccine

a. The stages of the bioprocess

The industrial *E. coli* culture process takes place in bioreactors. This process consists of a pre-culture phase in Erlenmeyer to amplify the quantity of cells contained in a frozen ampoule and to have enough biomass to seed the bioreactor. The bioreactor culture consists of 3 steps: Batch, Fed-batch and Fed-batch + induction.

- Batch phase: in this phase no additional feed (except the antifoam feed for pH regulation) is used from the beginning to the end of the phase: closed system. Indeed, all nutrients are present from the beginning. The main substrate present in the medium is glucose. It is therefore consumed by the cells, and it also leads to the production of acetate and lactate. This substance can acidify the medium, which is why it is important to control the pH of the system. In addition, oxygen consumption increases, causing a drop in the partial pressure of dissolved oxygen.

- Fed-batch phase: this phase starts when the substrate is completely consumed, adding substrate and supplements. In this way, there is an extension of the culture time to obtain higher cell densities. In this stage, the growth rate is controlled by a flow rate stipulated at the beginning of the Fed-batch medium feeding.
- Fed-batch and induction phase: once the quantity of biomass is reached, an induction is done by adding IPTG. This allows to produce the recombinant protein.

After a few hours after induction, the system is stopped, and the harvesting phase begins. In this phase, the culture is collected and purified to isolate the recombinant proteins. In addition, different analytical techniques are implemented to analyze the components present in the medium. These techniques will be described in *subsection c*.

b. Bioprocess control system

As previously presented, the amount of dissolved oxygen is an important parameter for the bioprocess. For this reason, the implementation of a pO_2 control system is necessary to ensure the optimal synthesis of the antigen [34]. The control system implemented in the *MenB coli* process is based on a PID (Proportional-Integral-Derivative) controller.

To be able to control the pO_2 , the system will act on the agitation and aeration variables. The control regulation system works in cascade because different variables will be manipulated [35]. This mode of operation uses a master controller that controls the actuators. In most cases, if the system requires oxygen, the control system will progressively increase the stirring speed to its maximum value. Once this value is reached, the system will increase the aeration rate to the maximum gassing set point. If

these two levers are not sufficient to maintain the pO_2 set point, the system engages the third lever which is the injection of pure oxygen at depth while maintaining the two previous levers constant.

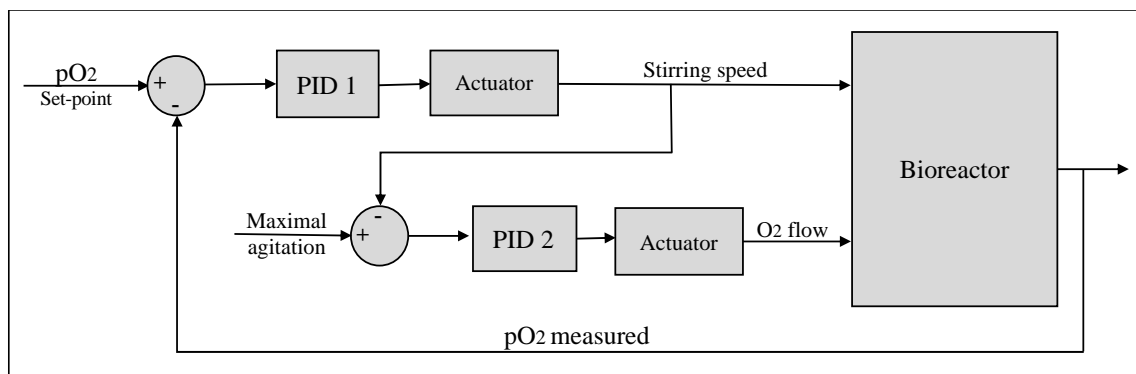
The system can also work in the opposite direction. If the oxygen supply is too high, the flow of pure oxygen will be reduced first, then the air aeration and finally the stirring speed. This regulation will act according to the pO_2 value set as a setpoint.

However, in most of the *MenB coli* culture trials, the air flow rate is taken out of the control (it is fixed throughout the culture), leaving the stirring speed and pure oxygen flow rate variables in the PID control. A general diagram of the operation is shown in

Figure 8.

Figure 8.

Block diagram of the PID control.



c. Analytical techniques

A recombinant protein production is a bioprocess that involves various key substances for its proper functioning. These include the necessary nutrients present in the environment, the biomass that can be produced and the amount of recombinant protein obtained. For this reason, it was necessary to use different analytical techniques.

The techniques implemented are:

- **Mass spectrometry:** the mass spectrometer is used as a gas analyzer. It allows the monitoring of gases leaving the bioreactor. The principle of analysis is based on the magnetic sector mass spectrometry by scanning [36]. This equipment works by ionizing a neutral gas sample, and the resulting charged particle components are separated according to their molecular weight. A detector then collects the ions of interest to scan and quantify the entire gas sample. The analyses allow calculations of O₂ consumption and CO₂ production by bacteria (OUR and CER). These values were required for the data treatment, as can be seen in the *equation (1)*.
- **UV-vis radiation spectrometry:** the spectrometer allows to measure the optical density of the cultures. This measurement is done at 600 nm against ultrafiltered water. The principle of operation is based on the interaction of a material with radiation that it absorbs. It is necessary to make dilutions for the samples to enter the measurement range (0,2 - 0,6) of the equipment. These values allow the calculation of biomass concentration by following *the equation (11)*.

$$X = d \cdot DO \tag{11}$$

Where, $X = \text{Biomass}$

$d = \text{dilution factor}$

$DO = \text{optical density}$

This technique was implemented to obtain the cell growth curves in each experiment. In this way, it was possible to evaluate if a similar curve is achieved when the scaling-down process took place.

- **HPLC:** High performance liquid chromatography (HPLC) is a technique used to separate and analyze proteins. It works in reverse phase because it is an organic gradient mode and follows the principles of adsorption and separation. HPLC has a non-polar phase (stationary) and a polar phase (mobile) [37]. In this way, this technique operates according to the principle of hydrophobic interactions. The

material of the separation column is silica (Ref. C18). Acetato nitrile is also required to increase the organic concentration that helps to extract the peaks (which are the most hydrophobic). Finally, the temperature set point was at 5°C to avoid a chemical reaction (blocks parasitic reactions). This technique was used to determinate antigen concentrations achieved in the experiments.

4.2.2. Case of study: scale-down of the MenB process

4.2.2.1. Selection of scale transposition criteria

A transposition criterion is all the parameters that are kept constant between the different scales. The two scales of interest in this study are 250 mL and 2 L, the Ambr250 and the Biostat respectively. The Ambr250 was chosen for this study because it allows to perform many experiments at the same time. The Biostat was chosen because the *E. coli* process has never been run in this bioreactor, so it is used as a proof of concept for a scale-down study "right the first time".

For Ambr250 bioreactor, to test the different transposition criteria, it was interesting to change the transposition criteria between each experiment and took different scales reference (**Table 2**). The two main scale references for these experiments were the 1000 L and 5 L bioreactors.

Table 2. Parameters established for scaling down on the Ambr250 bioreactor

Bioreactor	Reference scale	Transposition criteria
1	Reference Ambr250	-
2	Reference Ambr250	-
3	5 L	$k_{L,a}$ and vvm
4	1000 L	$k_{L,a}$ and vvm
5	100 L	$k_{L,a}$ and vvm
6	5 L	P/V and vvm
7	1000 L	P/V and vvm
8	1000 L	P/V and vvm

9	Reference Ambr250	Low CO ₂
10	-	Strong k _L a
11	-	Low k _L a
12	Control (feed*1,3)	Reference test

For the Biostat bioreactor, the transposition criteria was chosen by following the best results obtained in the Ambr250 bioreactor. In this way, according to the experiments and the literature [56], a good transposition process is obtained by using the best transposition criteria in the *MenB coli* process.

4.2.2.2. Scale transposition

First, a data search must be performed against previously performed *MenB coli* culture experiments in all bioreactors in the laboratory. Once the compilation of the data is done, the classification of the factors was implemented.

On the one hand, scale independent factors:

- Temperature, culture medium, pH control set point, pO₂ set point, and culture time.

On the other hand, the scale-dependent factors:

- The working and feed volume (Fed-batch), as well as the agitation and aeration parameters.

According to the methodology presented in **Figure 2**, the next step is the third one. The determination of the transposition criteria was done based on the literature and the different scale-up studies carried out by the fermentation team previously to this project, as well as the Ambr250 bioreactors experiments (*Case of study: scale-down of the MenB process section*).

Once the transposition criteria was identified, the transposition tool was implemented to determine the process conditions. It is necessary to fill in all the control

conditions applied to the reference scale (dependent and independent factors). After that, a Solver tool helped us to set the transposition criteria and find the new conditions.

4.2.2.3. Determination of oxygen volumetric transfer coefficient

a. Experimental determination

The experimental determination was based on the O₂ mass balance of the bioreactor (*equation (1)*). This determination focuses in the pO₂ regulation part to facilitate the estimations. As a result, the first term in *equation (1)* is deleted because the O₂ concentration remains constant. The equation is therefore the *equation (13)*.

$$OTR = OUR \quad (12)$$

$$k_L a (C_{O_2}^* - C_{O_2}) = OUR \quad (13)$$

The OUR values could be obtained from the extraction of the data from the gas analyzer (*see the Analytical techniques section*) or also by doing a mass balance. However, the system does not give direct values of dissolved oxygen concentrations. For this reason, they were calculated following Henry's law [39].

b. Theoretical determination

The theoretical determination follows the models that were found during the bioreactor's characterization. Thus, it was an independent equation for each scale that depends on the volumetric power input (P/V) and the linear gas velocity (U_g) [13]. However, as mentioned in *the Predictive models of the oxygen volume transfer coefficient section*, these models gives the behavior of the $k_L a$ in a medium that is considered as coalescent (water) due to the low salt concentration it contains. For this reason, it was essential to analyze these models under bacterial culture conditions. This medium is a non-coalescent medium because there are many dissolved elements such as glucose.

4.2. Models adaptation

Determining the "specific" factors of the culture media is an important step for model adaptation. This improves the predictive power of the models found in the coalescing media. It was first necessary to determine the influence of each coefficient in the equations. To do this, it was necessary to start from the characteristic equation of each bioreactor in order to linearize it. It was then essential to establish the independent and dependent variables of the equation to know the impact of the coefficient to be treated. Once the variables were calculated, the new value of the coefficient was found by setting up a linear regression. Taking into account *equation (14)* which presents the linearization of the general equation of $k_L a$. The **Table 3** shows the respective variables to be calculated according to the coefficient to be analyzed.

$$\ln(k_L a) = \ln(K) + a \cdot \ln\left(\frac{P}{V}\right) + b \cdot \ln(U_g) \tag{14}$$

Table 3. *Dependent and independent variables for linearization.*

Coefficient to be analyzed	Dependent variable (Y)	Independent variable (X)
K	$\ln(k_L a) - a \cdot \ln\left(\frac{P}{V}\right) - b \cdot \ln(U_g)$	$\ln(K)$
a	$\ln(k_L a) - \ln(K) - b \cdot \ln(U_g)$	$a \cdot \ln\left(\frac{P}{V}\right)$
b	$\ln(k_L a) - \ln(K) - a \cdot \ln\left(\frac{P}{V}\right)$	$b \cdot \ln(U_g)$

The comparison between the old and new values of the coefficients allowed the analysis of the influence of each of them. A large difference was reflected in a large impact in the equation, while a small difference may be even negligible. The factor focuses on the coefficient with the greatest impact. This factor was calculated as the ratio between the original value and the new value of the coefficient.

5. RESULTS AND DISCUSSION

5.1. Characterization of bioreactors

5.1.1. Results of the oxygen volume transfer coefficient

The experiments on the bioreactors were done in maximum volume (250 mL for the Ambr250 and 2 L for the Biostat). The DoE took into account the minimum and maximum values of most of the equipments (for some other bioreactors it was only taken into account the values applied in routine in the laboratory). The results of the k_La are presented in Table 4.

Table 4. Results of kLa in the Ambr250 and Biostat bioreactors

Bioreactor	N [rpm]	Qg [lpm]	$K_L a$ [h^{-1}]
Ambr250	249 - 4350	0,052 - 0,55	21 - 395
Biostat	21 - 1000	0,2 - 3,0	11 - 177

In this case, a comparison between bioreactors of similar geometry and operating conditions was done. For this reason, it was observed that the size of the bioreactor exerts an influence on the efficiency of the transfer of oxygen gas into the liquid medium. The highest coefficients are obtained in the Ambr250 bioreactor, i.e., better gas transfer for the smaller scale. This observation is consistent with previous work, in which we demonstrated that the smaller the bioreactor the more efficient is the gas transfer [13]. However, it is important to emphasize that the results are also related to the operating conditions applied to each bioreactor. Nevertheless, the great usefulness of the Ambr250 bioreactor is evident, besides being an automated equipment that can work with different bioreactors in parallel, it is verified that it achieves a good oxygen transfer in the experiments.

5.1.2. Statistical analysis of results

5.1.2.1. Volume transfer coefficient

Statistical analysis was performed using Excel and JMP. These two applications were used to evaluate the influence of each operation variable and their interactions, as described in section 4.1.1. The statistical parameter chosen for the analysis was the "*p-value*".

Table 5. Influence of operating conditions and their interactions in *k_L a* - *Ambr250*.

Source	LogWorth		P-value
N	4,962		0,00001
Qg	2,326		0,00472
N*N	0,953		0,11132
Qg*Qg	0,360		0,43619
N*Qg	0,317		0,48219

The

Table 5 presents the *p-value* values with respect to each operation variable studied and their interactions in the *Ambr250* bioreactor. A *p-value* greater than 0,05 indicates that there is not a great influence of the variable. In this case, we obtained that the agitation speed and aeration rate exert a great influence on the results of *k_L a*. In addition, agitation has a greater impact. However, the *p-value at the* interaction level is greater than 0,05. This indicates that there is not a great influence of the interactions of these variables.

The **Figure 9 (1)** shows a graphical representation of the impact of the variables. In these graphs the influence of the agitation speed was verified and a direct and linear behavior is observed on the transfer coefficient. The influence of the aeration is also direct, but the impact decreases at high aeration values.

The same analysis was done in the Biostat results. These results are shown in

Figure 9.

Influence of agitation and aeration rate in $k_L a$. (1) Ambr250 (2) Biostat

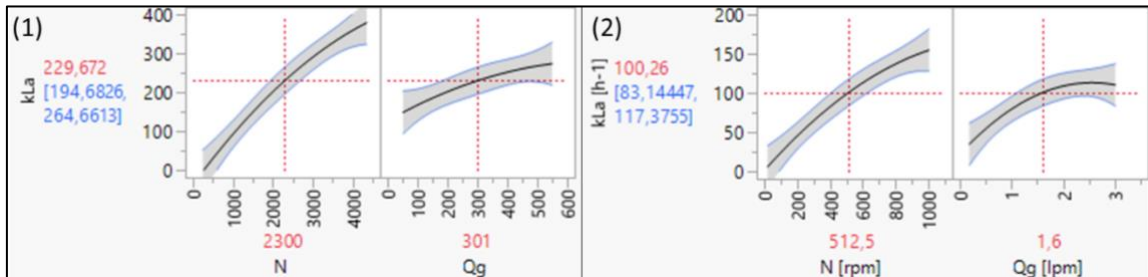


Table 6. The same impact was obtained in relation to that of the Ambr250 bioreactor. The *p-value* lower than 0,05 is obtained in the agitation speed and the aeration flow rate. In this case was also demonstrated that the agitation has a greater influence on the results of the $k_L a$. In addition, the behavior of these two study variables is linear in a large part of the condition values. Nevertheless, the slope is lower in the aeration flow (Figure 9 (2)).

Figure 9.

Influence of agitation and aeration rate in $k_L a$. (1) Ambr250 (2) Biostat

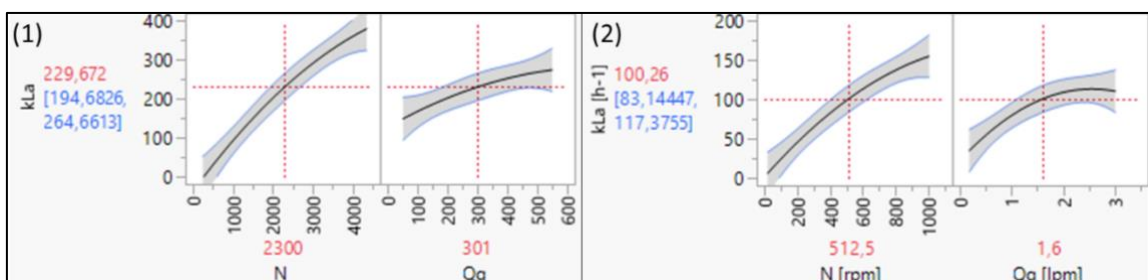


Table 6. Influence of operating conditions and their interactions in the $k_L a$ - Biostat.

Source	LogWorth	P-value
N	4,389	0,00004
Qg	2,777	0,00167

Source	LogWorth		P-value
Qg*Qg	1,341		0,04562
N*Qg	1,201		0,06302
N*N	0,923		0,11949

5.1.1.1. CO₂ Stripping

As previously presented, the study of CO₂ stripping was done by following the behavior of pH as a function of time. In this way, the response variable is "UpH/min". Once found the results, were put in the JMP application to analyze them. The analyses of the bioreactors Ambr250 and Biostat are presented in **Table 7** and **Table 8**.

Table 7. Influence of operating conditions and their interactions in UpH/min -

Ambr250

Source	LogWorth		P-value
Qg	4,804		0,00002
N	4,367		0,00004
N*N	2,911		0,00123
N*Qg	2,365		0,00432
Qg*Qg	1,198		0,06346

Table 8. Influence of operating conditions and their interactions in the

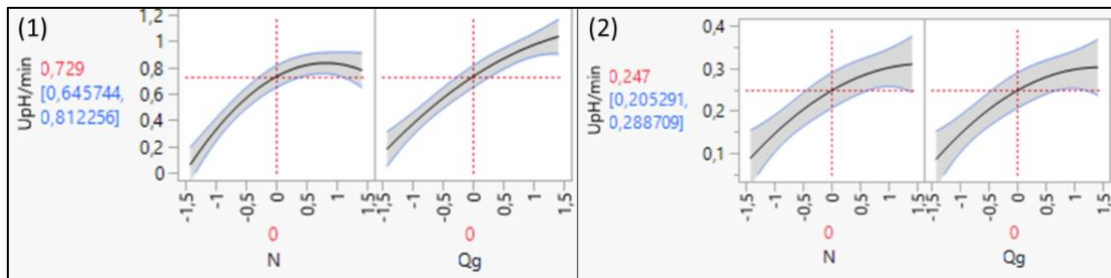
UpH/min - Biostat.

Source	LogWorth		P-value
N	3,191		0,00064
Qg	3,141		0,00072
Qg*Qg	1,014		0,09688
N*N	0,902		0,12529
N*Qg	0,184		0,65442

After performing the statistical analysis, we find that the influence of the previous two parameters (agitation and aeration) is also significant for CO₂ stripping . This is highlighted by the *p-value* of each operation variable (*p-value*<0,05), as well as the graph of its influence (**Figure 10**). The results of *UpH/min* in both bioreactors show a direct and linear behavior in almost the entire range of agitation and aeration values tested. In this case, the impact of the two variables is close.

Figure 10.

Influence of agitation and aeration rate in UpH/min. (1) Ambr250 (2) Biostat.



5.1.2. Predictive models

5.1.2.1. Oxygen volume transfer coefficient

Thanks to the data generated during our measurements of $k_L a$, mathematical models were built and these models allow to predict the values of $k_L a$ values corresponding to the control parameters applied to each bioreactor. Each bioreactor operates with different aeration conditions and agitation speed, and has its own geometry. It is therefore necessary to build a model for each of them.

As mentioned in *section 4.1.3*, the *equation (10)* is the starting point for the theoretical model of $k_L a$. This model depends strongly on the volumetric power input and the linear gas velocity, which is in good agreement with the control levers of $k_L a$ that were identified. The three coefficients (K, a, b) that are involved in the correlation have been calculated and are present in **Table 9**.

Table 9. *Coefficients of the theoretical correlation of $k_L a$.*

Bioreactor	K	a	b	average error
Ambr250	0,02	0,41	0,42	25%
Biostat	0,04	0,42	0,53	12%

The coefficients calculated for each bioreactor are of the same order of magnitude. These values are different for each bioreactor, but they have the same behavior in terms

of their influence on the $k_L a$. Indeed, the coefficient "b" which belongs to the linear aeration rate has a higher value than that of the volumetric power input. These observations were also made in previous works, when the results were compared to all the bioreactors that were characterized [13]. In addition, based on the average percentage of error, the model found for the Biostat bioreactor is lower.

After obtaining the descriptive coefficients for each bioreactor, a simulation was done in Matlab software to get a graph of the response surface of $k_L a$ as a function of agitation speed and aeration rate (APPENDIX VII). Graphs as a function of the volumetric power input dissipated in the aerated medium and the linear velocity of gas were also made. In this way, a more accurate idea of the results of the volume transfer coefficient with respect to oxygen in a range of the conditions used or the parameters could be obtained.

In addition, a comparison of the experimental and theoretical results of $k_L a$ was made. The results are presented in **Figure 11** and the **Figure 12**. From the analysis of these figures, the high descriptive level of the models are observed, as both slopes are close to unity. Similarly, the points of the values of $k_L a$ are close to the reference line ($Y=X$).

Figure 11.

Comparison of theoretical and experimental $k_L a$ results - Ambr250.

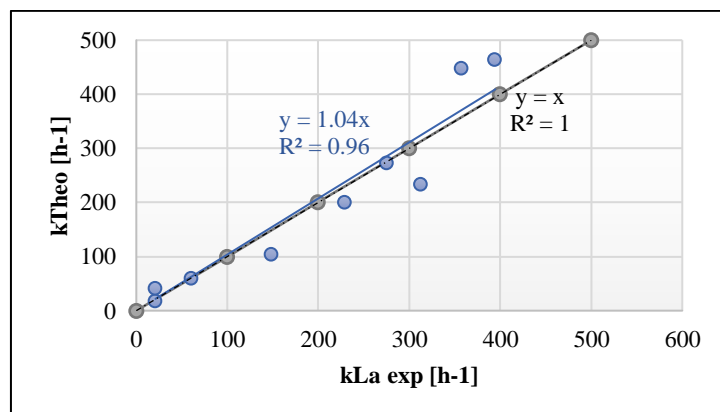
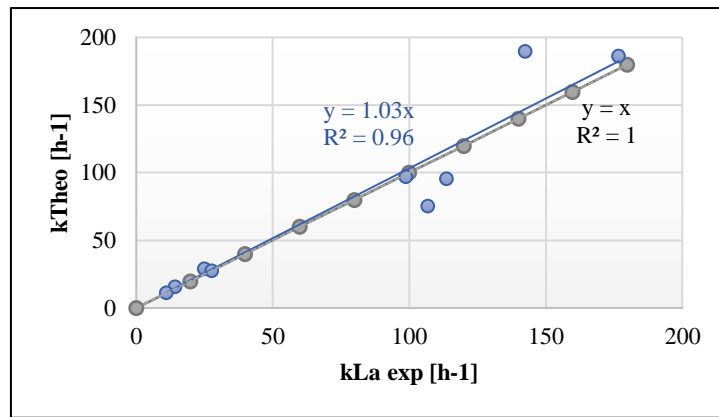


Figure 12.

Comparison of theoretical and experimental kLa results - Biostat.



The second model found was based on the response surface method used for DoE. These models also show a good level of prediction. However, it is important to point out that its complexity of use lies in the fact that it works with coded variables of the operating conditions (Agitation speed and aeration flow rate). The **Table 10** presents the coefficients found for each bioreactor, following the equation (15).

$$k_L a = A_0 + A_1 N + A_2 Q_g + A_3 N Q_g + A_4 N^2 + A_5 Q_g^2 \tag{15}$$

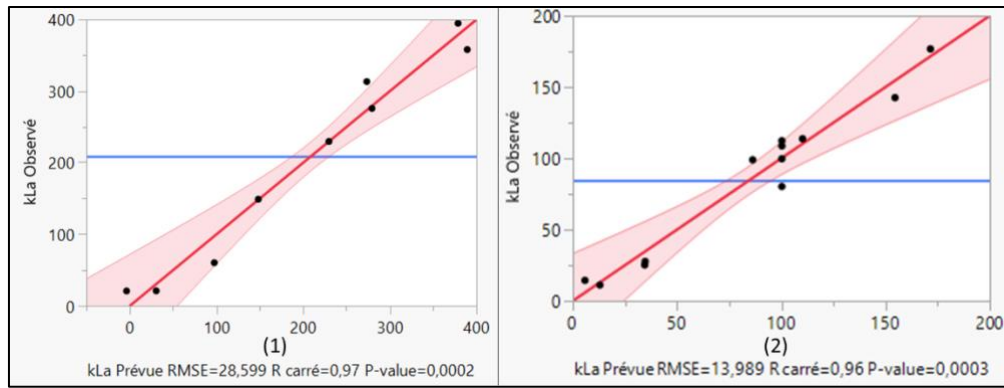
Table 10. *Coefficients of the statistical correlation of kLa.*

Bioreactor	A ₀	A ₁	A ₂	A ₃	A ₄	A ₅
Ambr250	230	135	44,2	10,7	-21,1	-9,44
Biostat	100	52,6	26,7	15,9	-10,0	-13,9

A comparison of the results given by this correlation with the experimental values was then made, using the JMP program. The obtained graphs are presented in **Figure 13**. In this way, the high level of prediction of the equations is confirmed.

Figure 13.

Comparison of statistical and experimental kL a results (1) Ambr250 (2) Biostat.



By making a comparison between the model based on the Van't Riet equation and the model found statistically, it is observed that both models achieve a good prediction of the k_La values. However, the use of the theoretical model is recommended because, besides not working with coded variables, it takes into account many parameters for its application (APPENDIX IV). It is important to note that these models decrease in performance at high values of k_La values. It would therefore be advisable to use the statistical model for values of $k_La > 350 \text{ h}^{-1}$ for Ambr250 and $k_La > 100 \text{ h}^{-1}$ for the Biostat.

5.1.2.2. CO₂ Stripping

The results of the pH monitoring units versus time for each bioreactor were used to complete the DoE and thus be able to have an equation based on the variables used. The coefficients found are therefore a function of the coded variables and their interactions (16).

$$UpH/min = B_0 + B_1 N + B_2 Q_g + B_3 N Q_g + B_4 N^2 + B_5 Q_g^2 \tag{16}$$

Table 11. Coefficients of the statistical correlation of UpH/min.

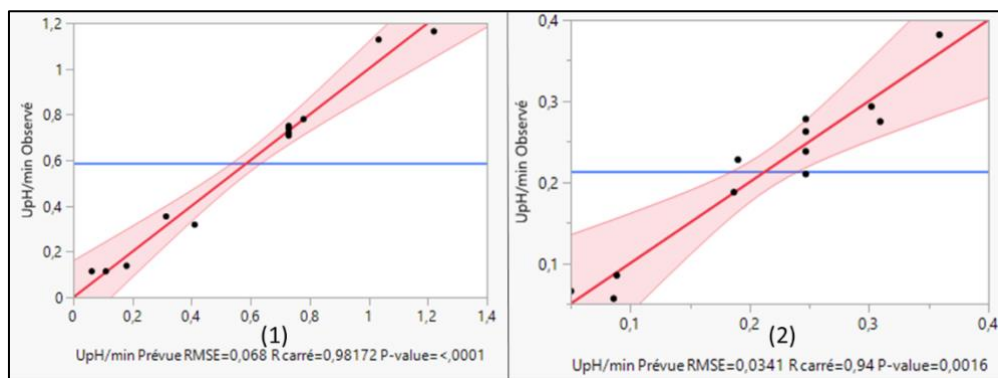
Bioreactor	B ₀	B ₁	B ₂	B ₃	B ₄	B ₅
Ambr250	0,729	0,253	0,302	0,152	-0,154	-0,061
Biostat	0,247	0,078	0,076	0,008	-0,024	0,026

By analyzing the results shown in **Table 11** is observed that there is a behavior in the coefficients depending on the size of the bioreactor. The highest coefficients correspond to the Ambr250 bioreactor. This observation has also been made in previous works [13]. Thus, the theory that the performance of CO₂ stripping is influenced by the bioreactor size is verified. These results were expected because the larger the bioreactor size, the greater the CO₂ accumulation.

By doing the same analysis that was done for the prediction of the $k_L a$ models, the **Figure 14**. shows a comparison between the experimental and theoretical CO₂ stripping results.

Figure 14.

Comparison of statistical and experimental UpH/min results (1) Ambr250 (2) Biostat.



The graphs show a good prediction of the models. It is observed that all the values of the coefficient of determination (R^2) are higher than 0,9. In the same way, it is observed that the points are close to the red line, which indicates a good level of accuracy of the values between the experimental value and the theoretical value. These results show

the high prediction that is obtained using the CCD method. Nevertheless, it is important to emphasize the greater complexity of the obtained models related to the use of coded variables.

5.2. MenB coli culture process

5.2.1. Culture

The MenB E. coli culture process is composed of a preculture and then a main culture consisting of 3 phases as described above: Batch, Fed-batch, Fed-batch + induction (not including the preculture). The total duration of the process is about 30 hours. The pre-culture performed in Erlen is incubated at 37 °C in a thermo-agitated oven. A sample is taken at the beginning of the culture for OD measurement and quantification of the quantity of initial cells, then at the end of the pre-culture to check that the OD at the end targeted by the process has been reached.

The main culture in bioreactor is monitored online by recording the process control parameters (pH, pO₂, rpm, etc...). Samples are also taken during the culture to measure the bacterial growth kinetics. The triggering of the different phases depends on the time and/or the OD according to the phases. The temperature, pO₂ and pH control loops are PID controlled.

5.2.1.1. Ambr250

Despite the fact that 12 experiments were performed with the Ambr250 system, we choose to present only 3 trials for the sake of clarity. This document will present three of them (*Bio 1 for the Ambr250 reference, Bio 3 for the 5 L bioreactor and Bio 7 for the 1000 L bioreactor*) as an example of the results obtained. During this test the pO₂, pH and temperature regulations were as expected. A peak of pO₂ is observed at about 8-10 h of batch culture. This behavior is normal and corresponds to a limiting substrate concentration at the end of the Batch phase marking the beginning of the Fed-batch phase.

The **Figure 15** shows the pO₂ behavior of the first bioreactor (process reference). The value of the air flow rate was changed manually twice, therefore, the pO₂ regulation was focused on the agitation and the O₂ flow rate. However, for the other bioreactors the sparger air injection is integrated in the pO₂ control loop and is managed through a PID control (cascade agitation, air flow and O₂ flow rate). This was done in order to have a larger range of data for model validation.

The **Figure 16** and the **Figure 17** show a different behavior of the pO₂ control loop. Indeed, although the value remains close to the set point (20%), we observe that agitation and aeration behave differently. The agitation speed in this case behaves exponentially, while the gas supply is linear.

It is interesting to note that the PID control is less fine when the system starts to inject pure oxygen, it is also from there that we observe regular excursions of the pO₂ below the control set point.

Figure 15.

Recording of process monitoring parameters throughout the experiment in bioreactor 1 (Ambr250).

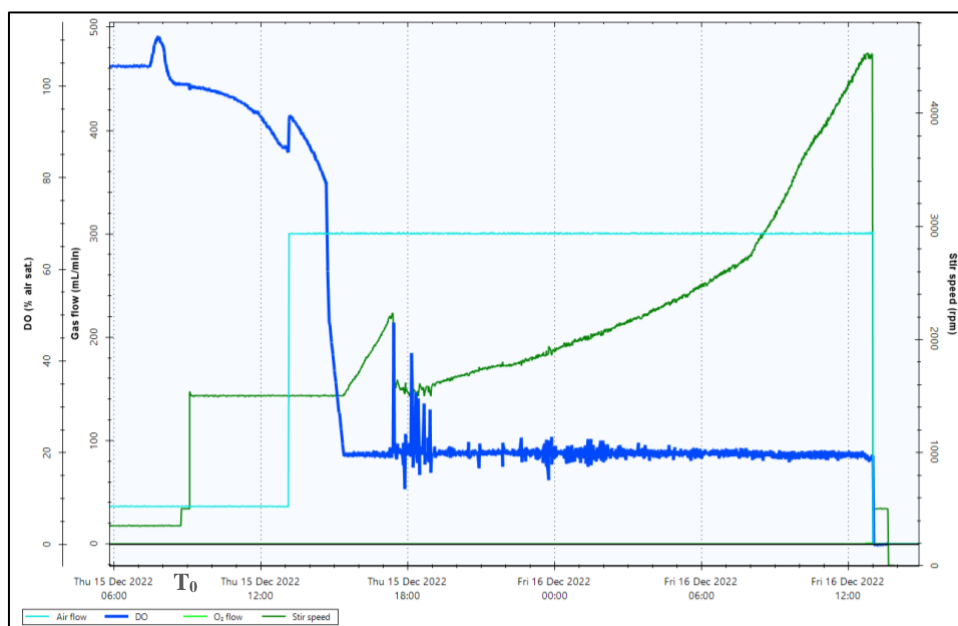


Figure 16.

Recording of process monitoring parameters throughout the experiment in bioreactor 3 (Ambr250).

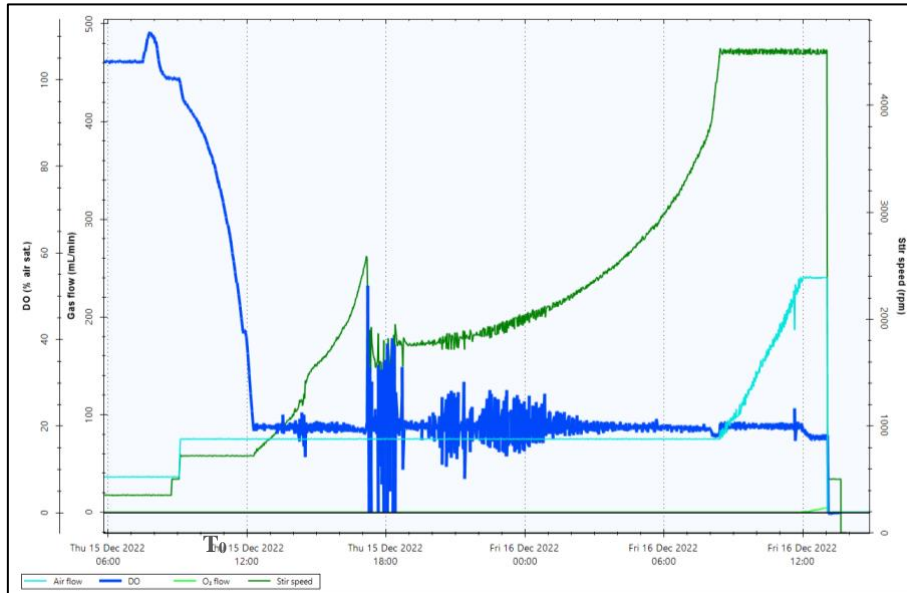
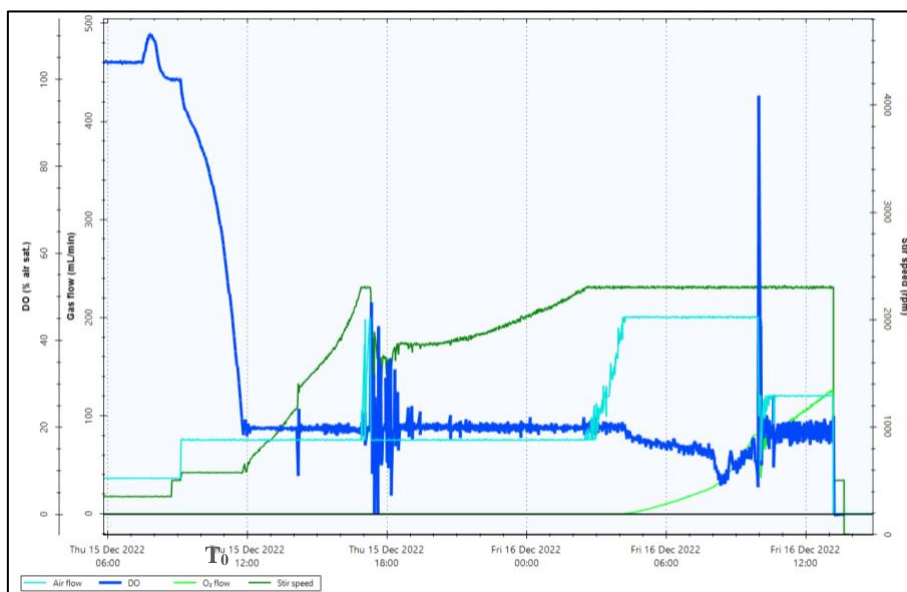


Figure 17.

Recording of process monitoring parameters throughout the experiment in bioreactor 7 (Ambr250).



A comparison of the profiles of the agitation and aeration conditions between the Ambr250 bioreactor 3 (same transposition criteria used for the Biostat) and the 5 L reference bioreactor was then made. Comparable profiles were obtained because the PID control acts on the conditions at the same time (approximately at $t=T_0+5h$ for agitation and $t= T_0 +25h (+/-2h)$ for O_2 flow rate), as well as the drop in agitation speed obtained at the start of the Fed-batch phase. *The APPENDIX VIII* presents all the profiles of the results of the 5 L reference bioreactor.

5.2.1.2. Biostat

In the Biostat bioreactor, only one experiment was performed due to the time available to finish the research project. For this reason, it was decided to work with a PID control equal to the one stipulated in the reference bioreactor (5 L). It is a regulation according to the agitation and the oxygen flow rate. The injection of air sparger is taken out of the pO_2 regulation loop and is managed via 2 different flow rates according to the stages of the cultures. The **Figure 18** and the **Figure 18** show the recording of the monitoring of the operating conditions, as well as the pO_2 .

Figure 18.

Recording of the process monitoring during culture of the Biostat experiment.

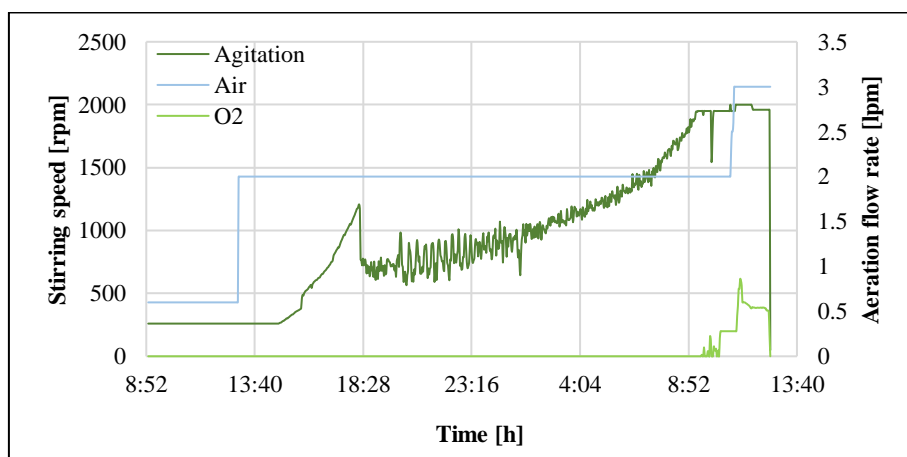
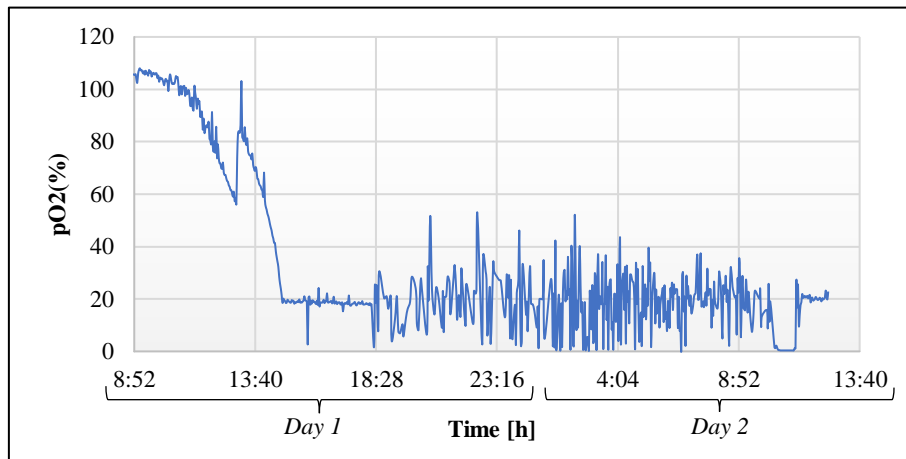


Figure 19.

Evolution of pO_2 throughout the Biostat experiment.



In the **Figure 19**, an excursion of pO_2 below the set point is observed (around 10:00 a.m. on day 2) accompanied by a period of several tens of minutes where the value was 0%. The cause of this excursion was the volume of the culture that exceeded the working volume of the bioreactor (2 L). The maximum volume was adjusted and the air flow rate was increased to bring the pO_2 back to its control value.

Regarding the pO_2 regulation, the **Figure 19** shows a profile with many oscillations that can be explained by the fact that this bioreactor has never been used for an *E. coli* culture before and therefore the PID parameters are not refined. These excursions can confound the $k_L a$ estimations. For this reason, a study of the internal parameters of the PID is necessary, so that it can have a better regulation.

The results of the agitation and aeration condition profiles were compared to those obtained for the 5 L reference bioreactor (**Figure 20 and Figure 21**). In both profiles it is observed that the agitation speed acts 5 h after the start of the batch phase. In addition, the aeration rate starts to act at the same time (about one hour after induction). This indicates comparable results between the three different scales.

Figure 20.

Comparison of stirring condition profiles between the Biostat and the 5L reference bioreactor.

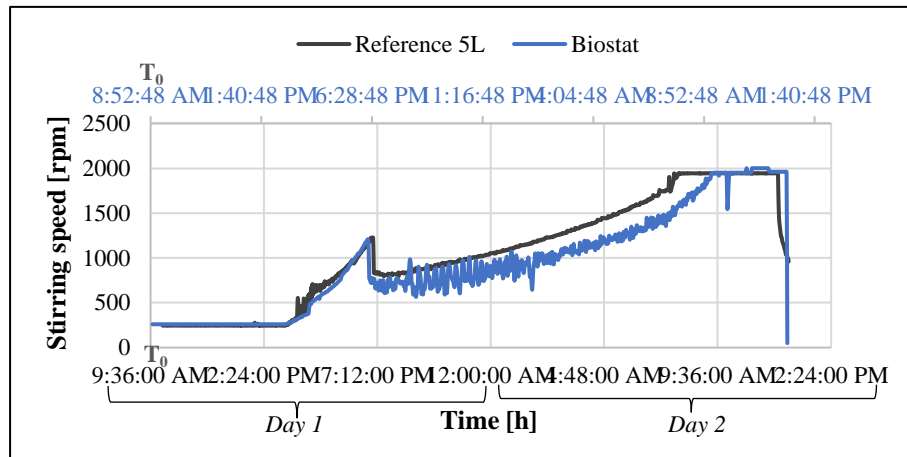
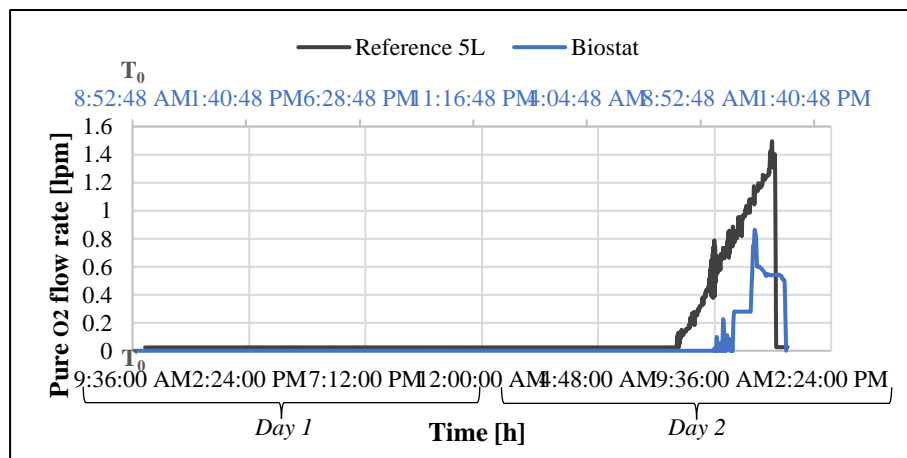


Figure 21.

Comparison of O₂ flow condition profiles between the Biostat and the 5L reference bioreactor.

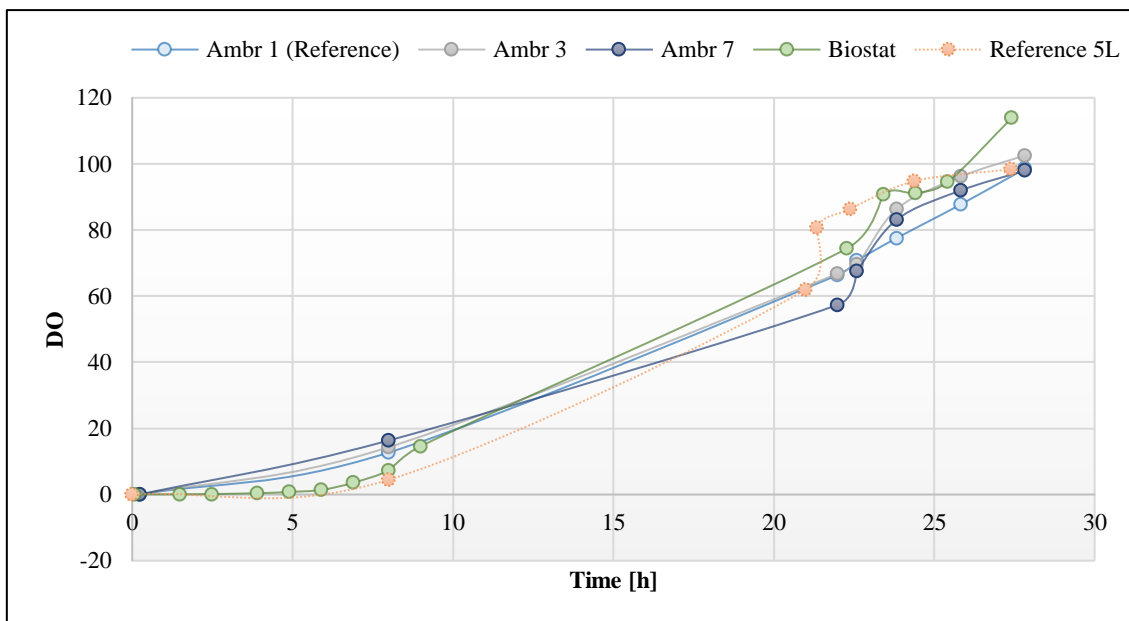


5.2.2. Biomass production

Samples were taken at different stages of the process to evaluate biomass growth. The **Figure 22** shows that good biomass production was obtained in the Ambr250 bioreactors and the Biostat.

Figure 22.

Cellular growth kinetics.



In the **Figure 22** was shown that the cell growth profile obtained is similar to the reference bioreactor. This indicates that having as transposition criteria the $k_L a$ and the vvm , a good performance of bacterial growth during transposition is obtained. Moreover, a higher cell density was obtained in the Biostat and this can be explained by the Fed-batch flow rate which underwent some adjustments related to the repriming of the injection pump several times. Indeed, during these repriming operations, a few extra milliliters of feed medium solution could be injected into the bioreactor.

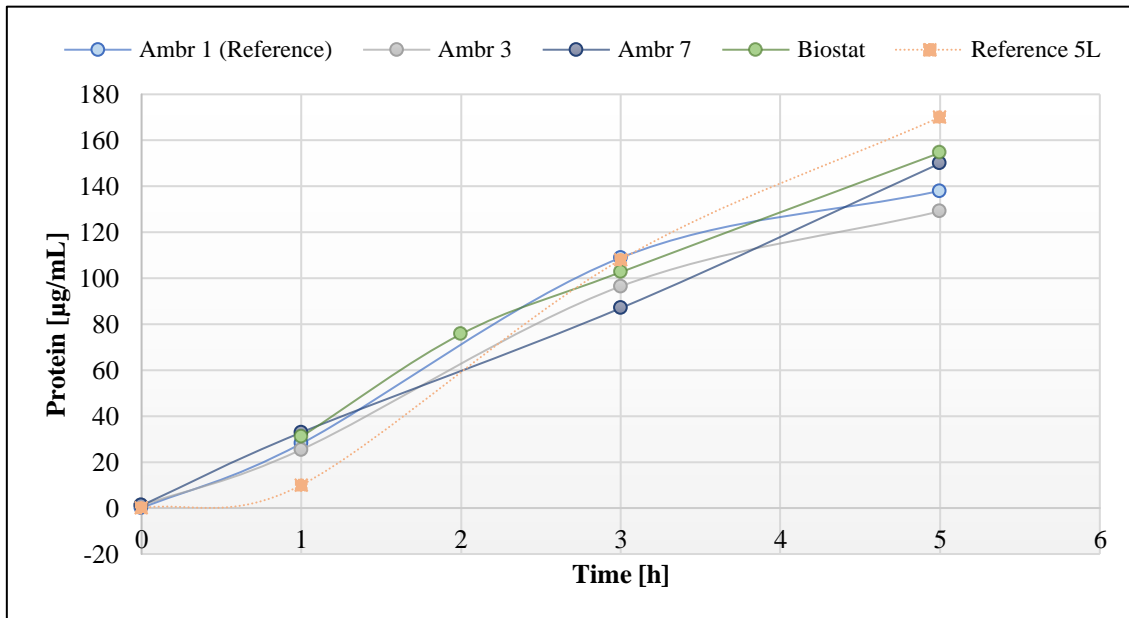
5.2.3. Antigen production

The concentration of antigen produced is calculated by the HPLC analysis technique. It was therefore performed cell lysis and pH shock to prepare the samples for

analysis. The **Figure 23** shows the results of four study bioreactors, as well as the reference bioreactor.

Figure 23.

Protein concentration profile.



It is observed that the protein production as a function of time is about 29 µg/mL per hour. This indicates that comparable profiles are obtained between the different scales. In addition, the Ambr250 bioreactor assays (7) and the Biostat achieved a final concentration similar to the reference (+/-10%). These results show a good performance compared to the reference bioreactor, even though each bioreactor was operated with different conditions. This indicates that an adequate transposition was performed and that the conditions found allowed to reach a good productivity.

Regarding the results of the Ambr250 bioreactors (1) and (3), the difference in productivity with the 5 L reference bioreactor is greater than 10%. However, the values presented remain within the range of productivity that has been presented in all laboratory tests (130-190 µg/mL). Moreover, the transposition made on Ambr 7 (transposition criteria: *P/V and vvm*) expect a better protein productivity compared to Ambr 1 (Reference). This indicates that these transposition criteria are good parameters for the

scale-down from 5 L to 250 mL. For this reason, it is important to evaluate the variation of other parameters to achieve equality in antigen production at all scales.

5.2.4. Oxygen volume transfer coefficient

The evaluation of the volumetric oxygen transfer coefficient was done in the Fed-batch phase of the process. In this phase, the PID control acts to keep the pO_2 value constant and equal to 20%. In this way, it is a steady state and therefore there is no variation of the oxygen concentration as a function of time. Indeed the $k_L a$ estimation is synthesized in *equation (15)*.

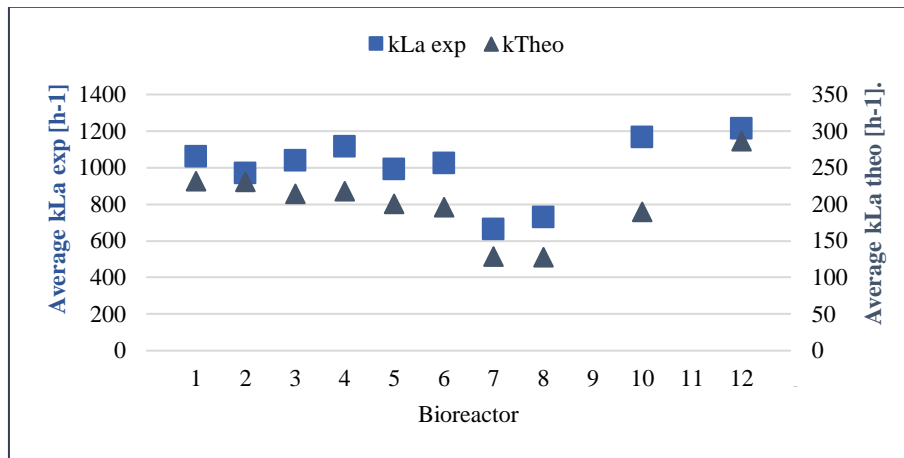
5.2.4.1. Ambr250

First, the calculations of the $k_L a$ were made. The $k_L a$ estimation was then calculated by following the theoretical equation found in *section 5.1.3*. For simplicity in the analysis of the results, the average of the $k_L a$ obtained in each bioreactor was calculated and these results are presented in **Figure 24**. It is important to emphasize that this figure presents all the 12 experiments done on the Ambr250 in order to make a comparison between them.

It is critical to note that bioreactors 9 and 11 were not processed because the gas analyzer did not operate and therefore data were not obtained. These were the bioreactors designed to maintain a constant air flow.

Figure 24.

Results of the average of experimental and theoretical $k_L a$ - Ambr250.



The graph presented above allows to see that although the same values of $k_L a$ are not obtained, they have the same relationship and trend in each of the bioreactors. However, it is evident that the theoretically calculated transfer coefficients are lower than the experimentally calculated ones. This result was expected since the models were characterized in a coalescent medium. Therefore, it is interesting to adjust the model, so that it can be used specifically for the *E. coli* culture.

5.2.4.2. Biostat

The same methodology of $k_L a$ estimation was performed in the Biostat bioreactor. The average of the $k_L a$ obtained is equal to 960 h⁻¹ and the average of the $k_L a$ theoretical to 480h⁻¹. In this way, it is verified the previous theory that tends to explain the difference between the theoretical and experimental models by the level of media coalescence. Moreover it also confirms the relationship between the quality of oxygen transfer and the size of the bioreactor, the smaller the bioreactor, the more efficient the transfer of material.

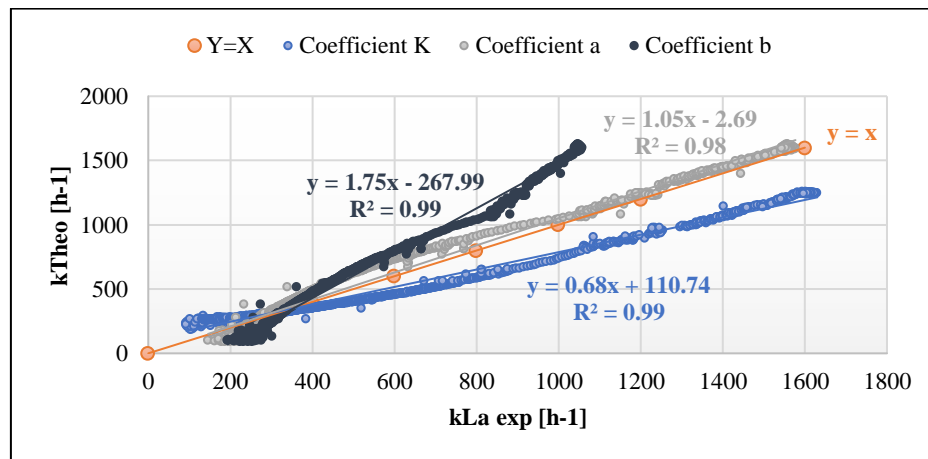
5.2.5. *Models validation*

5.2.5.1. **Ambr250**

The methodology used for the model adaptation was presented in *section 4.2*. The variation of each coefficient was evaluated holding the others constant. Once the adjusted coefficient was calculated, the new equation was applied to compare the results obtained with each modification. The results of the $k_L a$ obtained with the variation of each coefficient in bioreactor 3 are presented in **Figure 25**.

Figure 25.

Comparison of modified $k_L a$ models in bio 3 (Ambr250).



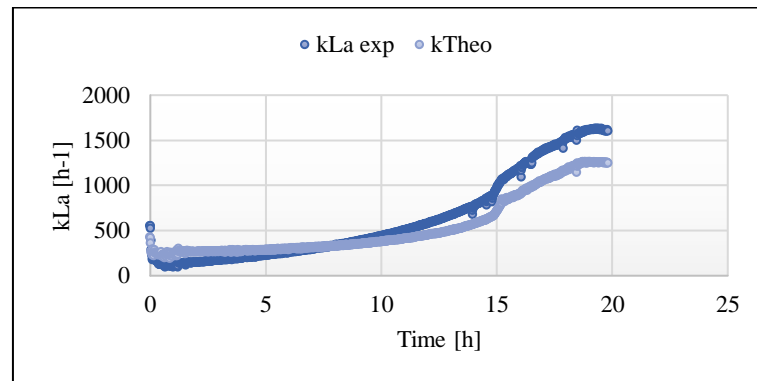
A value of the slope and the R^2 which is close to unity, indicates an approximation between the values of the abscissa and the ordinate. In other words, the closer they are to 1, the better the correlation. Moreover, another way to evaluate the good performance of the models is the proximity of the line $Y=X$. Indeed, it is observed in **Figure 25** that the best correlation is obtained when the *coefficient a* is modified.

This methodology was applied for all other Ambr250 experiments and the same impact was found with respect to the coefficients. For this reason, a multiplicative factor is then found for the coefficient with the most impact (*coefficient a*). The factor chosen is equal to **1.34** and was calculated from the average of the *coefficient a* of all bioreactors.

A comparison of the experimental and theoretical $k_L a$ experimental and theoretical values (modified correlation) is presented in **Figure 26**.

Figure 26.

$k_L a$ as a function of time in bio 3 (Ambr250).



The analysis of **Figure 26** indicates that after the adjustment of the model, the values of the data given by the latter can be considered as equivalent to those obtained experimentally.

5.2.5.2. Biostat

The same model adaptation methodology was performed in Biostat. However, the pO_2 regulation oscillated a lot throughout the experiment, which affects the evaluation and thus the adaptation of the model (*Section 5.2.1*). The results are presented in **Figure 27** and **Figure 28**.

Figure 27.

Comparison of modified $k_L a$ models in Biostat.

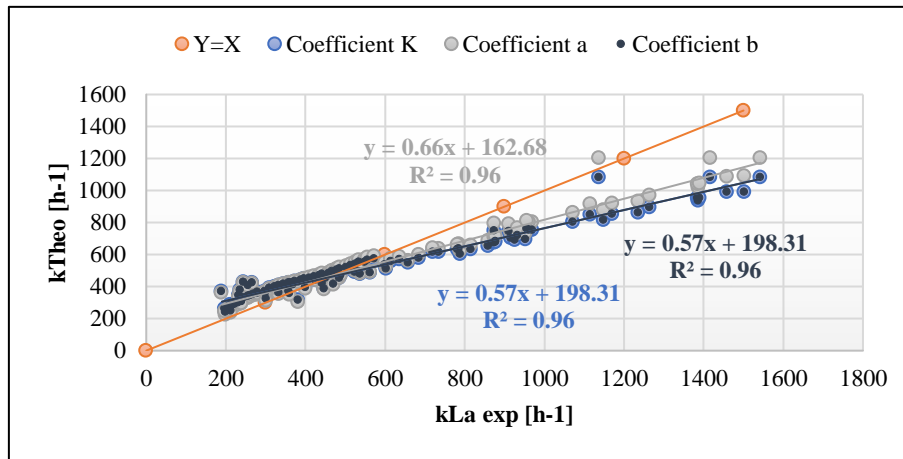
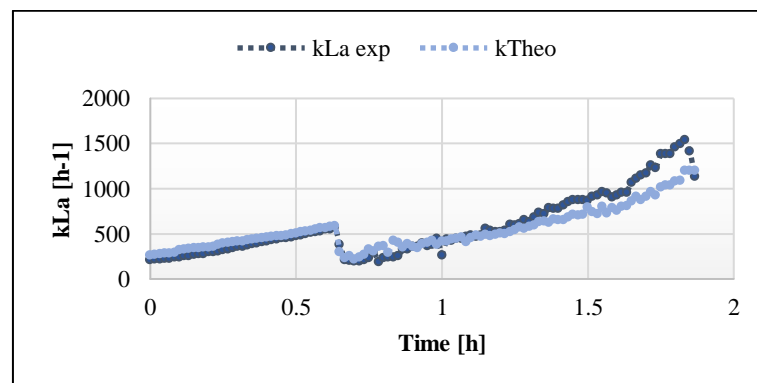


Figure 28.

$k_L a$ as a function of time in the Biostat.



The **Figure 27** shows that the best correlation was obtained when the "*a coefficient*" was modified (as for Ambr250). It is verified that the presence of microorganisms directly influences the power density. However, the value of the slope shows that the correlation found is not as powerful. This result may be related to the strong presence of oscillations during the regulation of pO₂. The **Figure 28** shows a comparison of the experimental and theoretical $k_L a$ experimental and theoretical values (modified correlation) with a factor found equal to **1.14**.

6. CONCLUSIONS AND PERSPECTIVES

Throughout this project, different experimental works were carried out in the fermentation pilot unit. These trials allowed the finalization of the last steps of the scaling tool project developed by the bacteriology team of the Mtech department. The methodology developed allows to simplify, harmonize and accelerate the scaling up studies of bioreactors. Indeed, the work described in this thesis shows that this methodology allowed to obtain a scale-down model quite representative of the reference scale (5 L), thanks to a theoretical pre-selection of the experimental conditions to be applied, in order to obtain a "right first time" result.

The bioreactors characterization in this project was done hydrodynamically using a sodium bicarbonate buffer solution (APPENDIX III) on the scales of 250 mL (Ambr250) and 2 L (Biostat). This characterization provided a descriptive model of the $k_L a$ and CO₂ stripping for each bioreactor. These models were added into the team's digital scale-up characterization tool. This has allowed the tool to progress, as well as having a dashboard to improve visualization and comparison of results.

Although the MenB process transposition was done for validation of the predictive power of the models and the tool, a model fit was required. This result is consistent because the characterization was done in a medium considered to be coalescent. Indeed, the culture medium is a constant parameter in the scaling of the processes. This evaluation allowed to identify the differences in gas transfer between the different scales. Similarly, it provided a potential explanation for the observed productivity differences.

Different perspectives were identified for improvement of the project. For example, increasing the maximum agitation value for the Biostat characterization. Although a good result was obtained, it could be improved if the maximum value of the

equipment is taken into account. Regarding the case study of the bacterial process, it is essential to perform a specific study on the descriptive parameters of the PID control. Despite the fact that the system tries to maintain its set point (20%), the irregularity of the set point maintenance may have affected the process and the model.

BIBLIOGRAPHIC REFERENCES

- [1] World Health Organization. *Covid-19 vaccines*. [Online]. Available from: <https://www.who.int/fr/emergencies/diseases/novel-coronavirus-2019/covid-19-vaccines>
- [2] Moreno, JA. *Scale-up of E. coli culture for optimal fed-batch strategy using exponential feeding*. Bionet Engineering. Spain.
- [3] Yawalkar, A. A., Heesink, A. B. M., Versteeg, G. F., & Pangarkar, V. G. (2002). *Gas-Liquid Mass Transfer Coefficient in Stirred Tank Reactors*. The Canadian Journal of Chemical Engineering, 80(5), 840-848.
- [4] Olmos, E. (2021). *Extrapolation of culture bioreactors*. Master 2 BioIN course. ENSAIA Biotech 3A.
- [5] Chevalot, I. (2019). *Methodological principles of extrapolation and intrapolation*. Master 2 BioIN ENSAIA Biotech 3A course.
- [6] Li J, Jaitzig J, Lu P, Süßmuth RD, Neubauer P. (2015). *Scale-up bioprocess development for production of the antibiotic valinomycin in Escherichia coli based on consistent fed-batch cultivations*. Microb Cell Fact. Jun 12; 14:83. DOI: 10.1186/s12934-015-0272-y. PMID: 26063334; PMCID: PMC4464625.
- [7] Kar, T. Delvigne, F. Destain, J. Thonart, P. (2011). *Bioreactor sizing and extrapolation based on physiological parameters: the case of lipase production by Yarrowia lipolytica*. Biotechnol. Agron. Soc. Environ. 15(4), 585-595.
- [8] Matsunaga, N., Kano, K., Maki, Y., & Dobashi, T. (2009). *Culture scale-up studies as seen from the viewpoint of oxygen supply and dissolved carbon dioxide stripping*. J. BIOSCI. BIOENG. 107(4, 412-418), 7. Thesis Dynamics of physiological response E. coli (s. d).
- [9] Tessier, L. (2018). *Stages of oxygen transfer*. [Online]. Shawinigan College, 2263 College Avenue, Shawiniigan, Quebec, Canada. Available at: <https://monde.ccdmd.qc.ca/>
- [10] Garcia-Ochoa, F., & Gomez, E. (2009). *Bioreactor scale-up and oxygen transfer rate in microbial processes: An overview*. Biotechnology Advances, 24 .
- [11] Zhang, X. (2019). *Systematic evaluation of high-throughput scale-down models for single-use bioreactors (SUB) using volumetric gas flow rate as the criterion*. Biochemical Engineering Journal, 9.

- [12] Hamilton. *Dissolved CO₂ series: Should CO₂ be a critical process parameter?* White paper. Hamilton Company.
- [13] Carreno Medina, NA. (2022). Scale-up. Characterization of bioreactors in the bacteriology area. Master 2 ENSAIA internship report. Sanofi.
- [14] Specialized authors Ooreka. Bacterial meningitis. [Online]. Available from: <https://migraine.ooreka.fr/>
- [15] Medicare. (2022). Meningitis: definition, causes, and circumstances of occurrence. [Online]. Available from: <https://www.ameli.fr/>
- [16] Sanofi. *Escherichia coli formation: expression system*. Available on: iLearn Sanofi.
- [17] My Vaccines. (2022). *Meningococcal B*. [Online]. Available from: <https://www.mesvaccins.net/>
- [18] Goergen, J. Guedon, E. Clincke, M. (2011). Processes for the production of therapeutic recombinant proteins: towards glycosylation control. DOI: [10.51257/a-v1-bio6200](https://doi.org/10.51257/a-v1-bio6200). BIO6200 v1.
- [19] Health & Medicine. Recombinant HB Vaccine production. [Online] Pharmaceutics. Available at: <https://eduhk.hk/biotech/eng/>
- [20] Akritidou, M. (2020). *The biotechnological Applications of E. coli*. [Online]. BioContact. Available at: <https://biocontact.ihu.edu.gr/the-biotechnological-applications-of-e-coli/>
- [21] Radio-Cadana.(2018). *E. coli: Infected romaine lettuce comes from California, FDA confirms*. [Online]. Available at: <https://ici.radio-canada.ca/nouvelle/1138267/>
- [22] Adouani, N. *Bioreactors and biocatalysts*. Course in the I2C specialization. 2A. ENSIC.
- [23] UGA Master of Biomanufacturing and Bioprocessing (2021). *Expression Systems*. [Online]. Available from: <https://www.youtube.com/watch?v=wEjka619zsQ>
- [24] New England Biolabs. *E. coli expression strains*. [Online]. Available from: <https://www.neb-online.fr/competent-cells/e-coli-expression-strains/>
- [25] Liege University. *Bacterial strains*. [On line]. Chapter 4.1. Available at: <https://orbi.uliege.be/bitstream/>
- [26] Institute of Technology and Science. (2015). *Response surface methodology*. Chapter 3. Statistical Inference and Applications course.
- [27] Koç B, Kaymak-Ertekin F. (2019). *Response surface methodology and food processing applications*. [Online]. Available from: <https://www.cabdirect.org/cabdirect/abstract/20103064527>

- [28] Ghoul, M. (n.d.). (2021). *Experimental and mixture designs*. 31. Master 2 course Industrialization of bioprocesses. ENSAIA Biotech 3A.
- [29] Bauer, I., Dreher, T., Eibl, D., Glöckler, R., Husemann, U., John, G. T., Kaiser, S. C., Kampeis, P., Kauling, J., Kleebank, S., Kraume, M., Kuhlmann, W., Löffelholz, C., Meusel, W., Möller, J., Pörtner, R., Sieblist, C., Tscheschke, B., & Werner, S. *Recommendations for process engineering characterisation of single-use bioreactors and mixing systems by using experimental methods (2nd Edition)*. 60.
- [30] Villemant, C. (2020) *ambr250 User's Manual*. Sartorius Stedim Biotech.
- [31] Sartorius Biotech (2020). *Univessel Glass. Reability and Continuity*. Simplifying Progress.
- [32] Sartorius Biotech (2020). *Biostat B. The Multi-talented bioreactor for research and development*. Simplifying Progress.
- [33] Van't Riet, K. *Review of measuring methods and results in nonviscous gas-liquid mass transfer in stirred vessels*. Ind. Eng. Chem. Process Des. Dev. vol. 18, No. 3, 1979.
- [34] Khan, O. Madhuranthakam, C. Douglas, P. Lau, H. Sun, J. Farrell, P. (2018). *Optimized PID controller for an industrial biological fermentation process*. ELSELVIER. DOI: 10.1016/j.jprocont.2018.09.007
- [35] Sanofi Pasteur. *Presentation pO₂ regulation Haemophilus influenzae type B (Hib) process*. Confidential information and property of Sanofi Pasteur.
- [36] Thermo Scientific. *Process mass spectrometry in biotechnology*. Process optimization at the speed of mass spectrometry.
- [37] Malviya, Rishabha & Bansal, Vvipin & Pal, Om & Sharma, Pramod. (2010). *High performance liquid chromatography: A short review*. *Journal of global pharma*. 2. 22-26.
- [38] Gonçalves, G. Prather, K. Monteiro, G. Duarte, M. (2014). *Engineering of Escherichia coli strains for plasmid biopharmaceutical production: Scale-up challenges*. ELSEVIER. Vaccine 32. 2847-2850.
- [39] Moulin, J. Pareau, D. Rakib, M. Stambouli, M. (2002). *Transfert de matière. Autres opérations compartimentées*. Techniques de l'ingénieur. J1074-1.
- [40] Fursy, R. (2012). *Validation of culture volume and fermentation parameters for Clostridium tetani toxoid production in the U4 fermenter*. Toulouse Laboratory. Department of Production Biology.
- [41] [Garcia-Ochoa, F. Gomez, E. Santos, V. Merchuk, J. \(2010\). Oxygen uptake rate in microbial processes: An overview. ELSELVIER. DOI: 10.1016/j.bej.2010.01.011](#)

- [42] [Protec Water treatment. *Solubility of oxygen in water as a function of temperature.* \[Online\]. Winkler's table. Available at: \[https://protec.pagesperso-orange.fr/22_Solubilite_de_l'oxygene.htm\]\(https://protec.pagesperso-orange.fr/22_Solubilite_de_l'oxygene.htm\)](https://protec.pagesperso-orange.fr/22_Solubilite_de_l'oxygene.htm)

APPENDIX
APPENDIX I

Scale transposition tool

Projet		Unité	Calculs et Corrélations
Design space	Paramètres		
X : paramètre process	Volume de milieu (V)	m ³	
X : Configuration bioreacteur	Diamètre du bioreacteur (D)	m	
Y : Configuration bioreacteur	Section interne du bioreacteur (Av)	m ²	$Av = \pi \cdot D^2 / 4$
Y : Configuration bioreacteur	Hauteur du milieu (h)	m	$h = V / Av$
Y : Configuration bioreacteur	Hauteur du milieu / Ø bioreacteur	m	h / D
X : Configuration bioreacteur	Hauteur du Fermenteur (H)	m	
Y : Configuration bioreacteur	Hauteur Ciel (hc)	m	$hc = H - h$
Y : Configuration bioreacteur	Ratio surface d'échange sur volume de milieu (R)	m ⁻¹	$R = Av / V$
Y : Configuration bioreacteur	Volume de ciel (Vc)	m ³	$Vc = Av \cdot hc$
Y : Configuration bioreacteur	Section maximum d'écoulement du gaz (S max)	m ²	$S_{max} = D^2 \cdot \pi / 4$
Y : Configuration bioreacteur	Section moyenne (S mean)	m ²	$S_{mean} = S_{max} / 2$
Y : Configuration bioreacteur	Périmètre de la section moyenne (P mean)	m	$P_{mean} = 2 \cdot \sqrt{S_{mean} \cdot (hc + h)}$
Y : Configuration bioreacteur	Diamètre hydraulique (Dh)	m	$Dh = 4 \cdot S_{mean} / P_{mean}$
X : paramètre standard	Viscosité Dynamique Milieu (μ)	Pa·s	
X : paramètre standard	Masse Volumique Milieu (ρ)	kg/m ³	
X : paramètre standard	Viscosité cinématique (ν)	m ² /s	$\nu = \mu / \rho$
X : paramètre process	Température de culture (T)	°C	
X : paramètre standard	Viscosité Dynamique air (μ_{air})	Pa·s	
X : paramètre standard	Masse Volumique air (ρ_{air})	kg/m ³	
X : paramètre standard	Diffusivité massique O ₂ dans air (D O ₂ /air)	m ² /s	
X : paramètre standard	Diffusivité massique CO ₂ dans air (D CO ₂ /air)	m ² /s	
X : paramètre milieu et gaz	Température gaz	°C	
X : paramètre process	Estimation RQ (RQ)		
Y : calcul intermédiaire	Estimation CER (CER est)	mmol/l/h	$CER_{est} = OUR_{est} \cdot RQ$
X : Configuration bioreacteur	Type sparger		
X : paramètre process	Débit d'air (Qg s)	l/h	
X : paramètre process	Débit O ₂ (Qg O ₂ s)	l/h	
X : paramètre process	Débit CO ₂ (Qg CO ₂ s)	l/h	
X : Configuration bioreacteur	Débit minimal		
X : Configuration bioreacteur	Débit max		
Y : caractérisation hydrodynamique	Volume de gaz / Volume de milieu / min (VVM)	min ⁻¹	$VVM = (Qg s + Qg O_2 s + Qg CO_2 s) / V$
X : paramètre process	Consigne surpression ciel (s)	bar	
Y : calcul intermédiaire	Débit total d'O ₂ entrant (Q O ₂ in)	mmol/h	$Q_{O_2 in} = (Qg O_2 s + Qg s \cdot 0,21) / 24,055$
Y : calcul intermédiaire	Consommation totale d'O ₂ (Q O ₂ cons)	mmol/h	$Q_{O_2 cons} = OTR \cdot V$
Y : calcul intermédiaire	Débit O ₂ sortant (Q O ₂ out)	mmol/h	$Q_{O_2 out} = Q_{O_2 in} - Q_{O_2 cons}$
Y : calcul intermédiaire	Estimation %O ₂ sortant (%O ₂ bubble out)	%	$\%O_2 \text{ bubble out} = Q_{O_2 out} / (Qg s + Qg O_2 s) \cdot 24,055$
Y : calcul intermédiaire	[O ₂] dissous à l'équilibre avec gaz sortant ([O ₂]in*)	mg/l	$[O_2]_{in}^* = (-0,1336 \cdot T + 11,605) \cdot (1+S) \cdot (\%O_2 \text{ bubble out} / \%O_2 \text{ air})$
Y : calcul intermédiaire	[O ₂] dissous à l'équilibre avec gaz entrant ([O ₂]in*)	mg/l	$[O_2]_{in}^* = (-0,1336 \cdot T + 11,605) \cdot (1+S + H^* \cdot 0,1) \cdot (\%O_2 \text{ entrant} / \%O_2 \text{ air})$
X : paramètre process	Consigne pO ₂ (pO ₂ sp)	%	
Y : calcul intermédiaire	[O ₂] dissous dans le milieu ([O ₂]l)	mg/l	$[O_2]_l = (-0,1336 \cdot T + 11,605) \cdot (1+S + H^* \cdot 0,1) \cdot pO_2 \text{ sp}$
Y : calcul intermédiaire	Différence de potentiel O ₂ global (moyenne logarithmique) ([O ₂]l* - [O ₂]l)	mmol/l	$[O_2]_l^* - [O_2]_l = ([O_2]_{in}^* - [O_2]_l) \cdot ([O_2]_{in}^* - [O_2]_l) / ([O_2]_{in}^* - [O_2]_l)$
Y : calcul intermédiaire	Différence de potentiel O ₂ global (moyenne simple) ([O ₂]l* - [O ₂]l)	mmol/l	$[O_2]_l^* - [O_2]_l = ([O_2]_{in}^* - [O_2]_l) / 2 + ([O_2]_{in}^* - [O_2]_l)$
X : paramètre process	Débit air surface (Qg ov)	l/h	
X : paramètre process	Débit azote surface (Qg N ov)	l/h	
X : paramètre process	Débit CO ₂ surface (Qg CO ₂ ov)	l/h	
Y : calcul intermédiaire	Vitesse linéaire gaz surface (U)	m/s	$U = (Qg ov + Qg N_2 ov + Qg CO_2 ov) / S_{mean}$
Y : calcul intermédiaire	Volume de gaz / Volume de milieu / min (VVM)	min ⁻¹	$VVM = (Qg ov + Qg N_2 ov + Qg CO_2 ov) / V$
Y : calcul intermédiaire	Volume de gaz / Volume de ciel / min (VVM ciel)	min ⁻¹	$VVM_{ciel} = (Qg ov + Qg N_2 ov + Qg CO_2 ov) / Vc$
Y : calcul intermédiaire	Débit CO ₂ entrant (Q CO ₂ in)	mmol/h	$Q_{CO_2 in} = (Qg CO_2 s + Qg CO_2 ov) / 24,055$
Y : calcul intermédiaire	Débit CO ₂ profondeur (Q CO ₂ p)	mmol/h	$Q_{CO_2 p} = CER_{est} \cdot V + Q_{CO_2 in}$
Y : calcul intermédiaire	Débit CO ₂ sortant (Q CO ₂ out)	mmol/h	$Q_{CO_2 out} = CER_{est} \cdot V + Q_{CO_2 in}$
Y : calcul intermédiaire	%O ₂ sortant (%O ₂ out)	%	$\%O_2 \text{ out} = (0,21 \cdot (Qg ov + Qg s) + Qg O_2 s - OTR \cdot V) / (Qg s + Qg O_2 s + Qg ov + Qg N_2 ov + Qg CO_2 ov) \cdot 24,055$
Y : calcul intermédiaire	Nombre de Reynolds (Re)		$Re = \rho \cdot U \cdot D / \mu$
Y : calcul intermédiaire	Nombre de Schmidt (Sc)		$Sc = \mu / (\rho \cdot D_{CO_2/air})$
Y : calcul intermédiaire	Coefficient de transfert de matière (CO ₂ dans l'air) en laminaire (K CO ₂)	m/s	$K_{CO_2} = 0,002 \cdot 0,664 \cdot Re^{0,5} \cdot Sc^{0,3} / D$
X : Configuration bioreacteur	Facteur de correction expérimental du coefficient de transfert (C1)		
X : Configuration bioreacteur	Kla CO ₂ surface (Kla CO ₂)	h ⁻¹	$Kla_{CO_2} = K_{CO_2} \cdot CO_2 / C^* \cdot Av / V$
Y : caractérisation hydrodynamique	pCO ₂ si pas de gaz surface (pCO ₂ wov)	%	$pCO_2 \text{ wov} = Q_{CO_2 out} / (Qg s + Qg O_2 s + Qg CO_2 s) \cdot 24,055$
Y : caractérisation hydrodynamique	pCO ₂	%	$pCO_2 = (Q_{CO_2 p} + V \cdot K_{CO_2} \cdot \%CO_2 \text{ out}) / (Kla_{CO_2} \cdot V + Qg s + Qg O_2 s + Qg CO_2 s)$
Y : calcul intermédiaire	Débit de CO ₂ strippé en surface (Q CO ₂ ss)	mmol/h	$Q_{CO_2 ss} = K_{CO_2} \cdot C^* \cdot (pCO_2 - \%CO_2 \text{ out}) / 24,055 \cdot V$
Y : calcul intermédiaire	Débit de CO ₂ strippé en profondeur (Q CO ₂ sp)	mmol/h	$Q_{CO_2 sp} = pCO_2 \cdot (Qg s + Qg O_2 s + Qg CO_2 s) / 24,055$
Y : calcul intermédiaire	Pression de CO ₂ dissous en mmHg	mm Hg	$p_{CO_2} = pCO_2 \cdot 760$
Y : calcul intermédiaire	[CO ₂] dissous dans le milieu ([CO ₂]l)	g/l	$[CO_2]_l = (-0,0357 \cdot T + 2,3785) \cdot (1+S + H^* \cdot 0,1) \cdot pCO_2$
X : Configuration bioreacteur	Type de mobile d'agitation		
Y : Configuration bioreacteur	Ø bioreacteur / Ø mobile	m	D / d
X : Configuration bioreacteur	Diamètre du mobile d'agitation (d)	m	
X : Configuration bioreacteur	Nombre de puissance du mobile (Np)		
X : Configuration bioreacteur	Nombre de pompage du mobile (Nm)		
X : Configuration bioreacteur	Remarques sur mobiles d'agitation		
X : paramètre process	Nombre de mobiles immergés (Nm)		
X : paramètre process	Vitesse d'agitation (RPM)	min ⁻¹	
X : Configuration bioreacteur	Vitesse d'agitation minimale (rpm)	min ⁻¹	
X : Configuration bioreacteur	Vitesse d'agitation maximale (rpm)	min ⁻¹	
Y : caractérisation hydrodynamique	RPS (N)	s ⁻¹	$N = RPM / 60$
Y : caractérisation hydrodynamique	Nombre de Reynolds (Re)		$Re = \rho \cdot N^2 \cdot d^2 / \mu$
Y : caractérisation hydrodynamique	Nombre de Froude (Fr)		$Fr = N^2 \cdot d / g$
Y : calcul intermédiaire	Débit de pompage (Qp)	m ³ /s	$Q_p = Nm \cdot N^2 \cdot d^3$
Y : calcul intermédiaire	Temps de cycle (tc)	s	$tc = V / Q_p$
Y : caractérisation hydrodynamique	Temps de médiane (tm)	s	$tm = tc \cdot 3$
Y : calcul intermédiaire	Puissance dissipée par agitation (Pa)	W	$Pa = Np \cdot \rho \cdot N^3 \cdot d^5 \cdot Nm$
Y : calcul intermédiaire	Puissance dissipée par gaz (Pg)	W	$Pg = \rho \cdot V \cdot U^3 \cdot 9,81$
Y : calcul intermédiaire	Puissance volumique totale dissipée (P/V)	W/m ³	$P/V = (Pa + Pg) / V$
Y : caractérisation hydrodynamique	Puissance volumique totale dissipée en milieu aéré (P/V)g	W/m ³	$(P/V)g = ((1,12 \cdot 6^N) \cdot Pa + Pg) / V \cdot Na < 0,035$
Y : caractérisation hydrodynamique	Couple	N/m	$(P/V)g = ((1,12 \cdot 6^N) \cdot Pa + Pg) / V \cdot Na > 0,035$
Y : caractérisation hydrodynamique	Vitesse en bout de pale (Vp)	m/s	$Vp = \pi \cdot N \cdot d$
Y : caractérisation hydrodynamique	Echelle moyenne de Kolmogorov (lk moy)	µm	$lk_{moy} = ((\mu / \rho) / 3)^{1/4} / (P/Vg)^{1/4}$
Y : caractérisation hydrodynamique	Echelle min de Kolmogorov (lk min)	µm	$lk_{min} = ((\mu / \rho) / 10)^{1/4} / (P/Vg)^{1/4}$
Y : caractérisation hydrodynamique	Caillagelement (G)	s ⁻¹	$G = (P/Vg) / \mu^{0,5}$
Y : caractérisation hydrodynamique	Contrainte turbulente (Tn)	mmole	$Tn = (P/Vg) \cdot d / (6,5 \cdot \mu)^{0,75}$
Y : calcul intermédiaire	Vitesse superficielle de gaz (Ug)	l/h	$Ug = (Qg s + Qg O_2 s) / Av$
Y : caractérisation hydrodynamique	Nombre d'aération (Na)		$Na = (Qg s + Qg O_2 s) / (N^2 \cdot d^3)$
Y : caractérisation hydrodynamique	Limite de dispersion des gaz (Nc)		$Nc = 0,2 \cdot (d/D)^{0,5} \cdot Fr^{0,5}$
Y : caractérisation hydrodynamique	Kla selon la corrélation de Van't Riet 1979	h ⁻¹	$Kla = 0,002 \cdot (Pg/V)^{0,7} \cdot Ug^{0,2}$
X : Configuration bioreacteur			
X : Configuration bioreacteur	Kla selon l'étude de caractérisation pour chaque échelle de la zone de fermentation	h ⁻¹	Spécifique en fonction des équipements
Y : caractérisation hydrodynamique			
Y : caractérisation hydrodynamique	OTR (Viable si faible conso d'O ₂)	mmol/l/h	$OTR = Kla \cdot ([O_2]_{in}^* - [O_2]_l)$
Y : caractérisation hydrodynamique	Oxygène transfert rate (OTR)	mmol/l/h	$OTR = Kla \cdot ([O_2]_{in}^* - [O_2]_l)$
Y : caractérisation hydrodynamique	Stripping de CO ₂ selon l'étude de caractérisation pour chaque échelle de la zone de fermentation	Uph/min	Spécifique en fonction des équipements. Équation statistique : utilisation des variables codées.

Screenshot of the scale transposition tool

Bioreacteurs		Limites des conditions d'opération			Conditions			Paramètres			Résultats		
Numéro	Type bioreacteur	Volume de culture min. - max. [L]	Debit d'air [l/min]	Volume de culture [l]	Volume de culture [l]	Debit d'air [l/min]	Debit d'air [l/min]	Puissance volumique [W/m ³]	Puissance linéaire de gaz [W/m]	VVM [min ⁻¹]	M.a [h]	OTR [1/h]	OTR [1/h]
1	Arhe 200	0.05	0.05-0.05	0.05	0.05	0.05	0.05	0.05	0.05	0.41	23	0.05	0.05
3	Biorat	10-20	0.2-3	10-20	15	260	0.00	0.00	0.00544	0.41	23	0.00	0.00
4	Foljatch	3.7-5.5	0.5-8	3.7-5.5	3.7	300	1.00	0.00	0.00190	0.41	23	0.00	0.00

kLa & stripping CO2

This bar chart compares the oxygen transfer coefficient (kLa) and CO2 stripping rate for three bioreactors. The y-axis represents kLa [1/h] from 0 to 25. The x-axis lists the bioreactors: Core microcell, Bioreacteur, and P51. Values are: Core microcell (0.48), Bioreacteur (0.83), and P51 (0.84). A red arrow indicates the 'Optimum' at 0.84.

PV & VVM

This bar chart compares the power input (PV) and volumetric gas velocity (VVM) for three bioreactors. The y-axis represents PV [W/m³] from 0 to 200. The x-axis lists the bioreactors: Core microcell, Bioreacteur, and P51. Values are: Core microcell (187), Bioreacteur (124), and P51 (100). A red arrow indicates the 'Debit de gaz volume de milieu' at 0.41.

OTR & VVM

This bar chart compares the oxygen transfer rate (OTR) and volumetric gas velocity (VVM) for three bioreactors. The y-axis represents OTR [1/h] from 0 to 4.0. The x-axis lists the bioreactors: Core microcell, Bioreacteur, and P51. Values are: Core microcell (3.5), Bioreacteur (3), and P51 (3). A red arrow indicates the 'Debit de gaz volume de milieu' at 0.41.

APPENDIX II

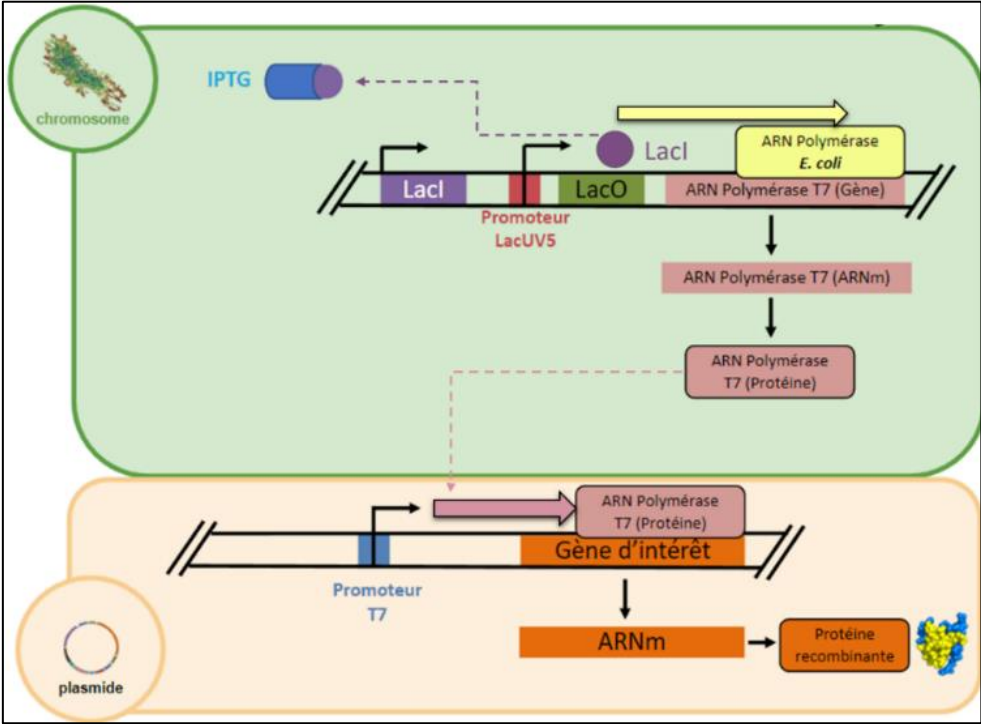
Production process of the recombinant protein

The production of a recombinant protein is done by cloning recombinant DNA using *E. coli* strains. This process is a gene expression vector system. The vector is also called a plasmid and carries the gene of interest.

In this system, the T7 RNA polymerase is used and binds specifically to its associated T7 promoter, which is a strong promoter. For this reason, once the T7 promoter is inserted into a plasmid, many copies of the T7 RNA polymerase are produced and allows the transcription of the gene of interest [23].

The T7 RNA polymerase gene itself is encoded in the genome of certain genetically modified *E. coli* strains and is controlled by a Lac promoter. As a result, the LacI repressor protein binds to an operator sequence just downstream of the promoter, preventing transcription of the T7 RNA polymerase gene, and thus production of the target protein encoded by the plasmid. This transcriptional inhibition can be regulated by different compounds. An example of this is IPTG (Isopropyl β -D-thiogalactopyranoside), which causes a conformational change in the LacI protein preventing it from binding to the T7 promoter and thereby allowing the expression of the T7 RNA polymerase gene and consequently of the gene of interest whose expression is directly dependent on the presence of T7 RNA polymerase. Unlike the natural repressor, IPTG is not hydrolyzed by the enzyme beta-galactosidase, so it reliably allows protein expression when added to *E. coli* cultures. For further understanding, the **Figure 29** shows a schematic of the process.

Figure 1.
Recombinant protein process.



APPENDIX III**Buffer solution description sheet**

Topic: Preparation of sodium bicarbonate buffer [40].

Material:

1. Sodium bicarbonate (2.8 g/L).
2. Hydrochloric acid (36%).
3. Water.

Method:

1. The bioreactor is filled with water according to the desired working volume.
2. Powdered anhydrous sodium bicarbonate is introduced into the bioreactor with the aim of having a concentration of 2.8 g/L.
3. Stirring is started at a speed sufficient to dissolve the salt and obtain a good homogeneity.
4. After dissolution the pH of the solution is around 9.0
5. Hydrochloric acid is used to adjust the pH to 7.0.
6. The solution is ready to start the experiments.

Note: The interest of using a sodium bicarbonate solution is to be able to follow the evolution of dissolved O₂ and pH at the same time. The evolution of the pH is proportional to the elimination of dissolved CO₂. This technique allows to follow at the same time the transfer of O₂ in the medium and the stripping of CO₂.

APPENDIX IV

Parameters and equations for bioreactor sizing

The knowledge of the geometrical data of the bioreactors is necessary for the good dimensioning and characterization. First of all, the following data must be measured or extracted from the supplier:

Table 12. Bioreactor data.

Bior	Parameter	Ambr250	Biostat	Polybatch
	Number of power (N_p)	3,7	4,5	5
	Density water (ρ_L)	1000 Kg.m ⁻³	1000 Kg.m ⁻³	1000 Kg.m ⁻³
	Diameter of the tank (D)	0,06 m	0,153m	0,153m
	Number of agitators (N_m)	2	2	3
	Diameter of the agitator (d)	0,02 m	0,05	0,05

Once the recompilation of the data is done, the Reynolds number must be calculated to determine the fluid flow regime.

$$Re = \frac{\rho \cdot N \cdot d^2}{\eta}, \text{ si } Re > 10^4 \text{ turbulent}$$

$\rho =$ masse volumique du fluide agité [Kg/m³]

$N =$ vitesse d'agitation [tour/s]

$d =$ diamètre du mobile d'agitation[m]

$\eta =$ viscosité du fluide [Pa · s]

A turbulent regime allows to intensify the operations of transfer of matter, heat and momentum. In this way, the calculations are simplified compared to other flow regimes. This being the case, the power density in aerated medium. Indeed, it is a basic parameter of operation because the greater the power, the greater the intensity of transfer operations will be [7]. Its calculation is done according to the following equations:

1. Power dissipated by the agitation $P_a = N_p \cdot \rho_L \cdot N^3 \cdot d^5 \cdot N_m$

2. Linear gas velocity

$$U_g = \frac{Q_g}{A} = \frac{Q_g}{\pi \cdot D^2 / 4}$$

3. Power dissipated by the gas

$$P_g = \rho_L \cdot V_L \cdot U_g \cdot g$$

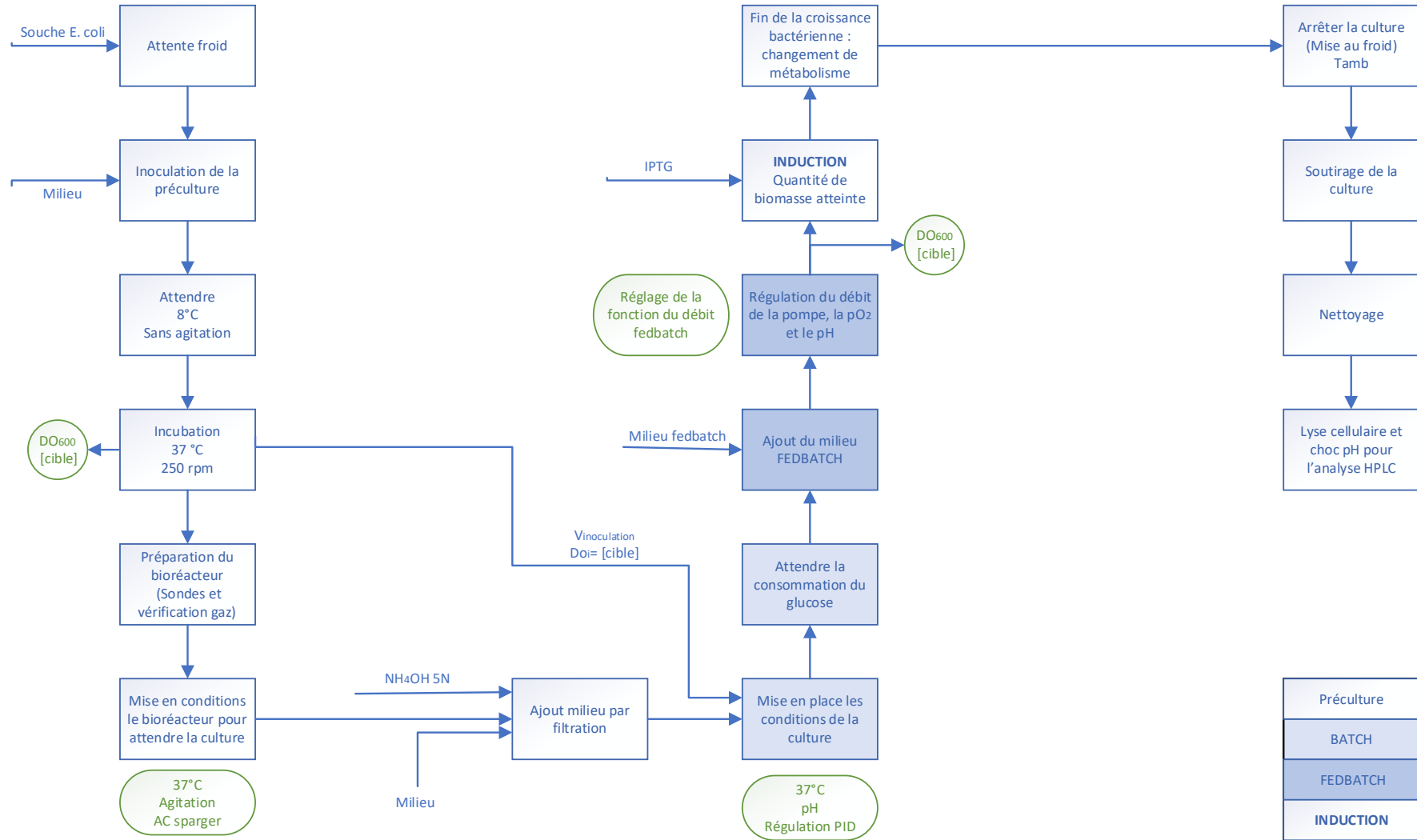
4. Number of aeration

$$N_a = \frac{Q_g}{N \cdot d^3}$$

5. Aerated dissipated power density $Si N_a < 0,035 \rightarrow \frac{P_g}{V_L} = \frac{(1-12,6 \cdot N_a) \cdot P + P_g}{V_L}$

6. $Si N_a > 0,035 \rightarrow \frac{P_g}{V_L} = \frac{(0,62-1,85 \cdot N_a) \cdot P + P_g}{V_L}$

APPENDIX V - Block diagram for the MenB coli culture process



APPENDIX VI

Determination of the experimental $k_L a$ in the presence of microorganisms

Obtaining the equation that allows the calculation of the experimental $k_L a$ in the presence of microorganisms is described in *section Error! Reference source not found.*. It is thus necessary to start from *equation (15)* to follow after the equations presented below.

$$k_L a_{O_2} = \frac{OUR}{(C_{O_2}^* - C_{O_2})}$$

1. Oxygen consumption by the cells (OUR)

Normally the bioreactors and/or gas analyzers give the value of OUR. It is therefore necessary to pay attention to the units of measurement to have an equality of units. However, the OUR value can be calculated by doing a material balance as follows [41]:

$$OUR = r_{O_2}''' = \frac{Q_{g,in}^{O_2}}{V} (y_{O_2}^{in} - y_{O_2}^{out})$$

2. Oxygen concentration gradient ($C_{O_2}^* - C_{O_2}$)

For the calculation of the oxygen concentration in saturation, it is necessary to know first the concentration that enters and leaves the medium. For this reason, these concentrations depend strongly on the gas that is used to bring oxygen to the system. In this case, Henry's law is implemented [39]. Similarly, Winkler's correlation is used to have the solubility of oxygen in water as a function of the temperature of the system [42]:

a. Saturation oxygen concentration:

$$O_2^* = (-0,1336 \cdot T + 11,605) * (1 + P_{ciel} + h \cdot 0,1)$$

$$C_{O_2,in}^* = O_2^* \cdot \frac{\left(0,21 \cdot \frac{Q_g^{Air}}{Q_g^{Air} + Q_g^{O_2}} + 1 \cdot \frac{Q_g^{O_2}}{Q_g^{Air} + Q_g^{O_2}} \right)}{0,21}$$

$$C_{O_2,out}^* = (-0,1336 \cdot T + 11,605) \cdot (1 + P_{ciel}) \cdot \frac{y_{O_2}^{out}}{y_{O_2}^{in}}$$

$$C_{O_2}^* = \frac{C_{O_2,in}^* + C_{O_2,out}^*}{2}$$

b. Oxygen concentration in the medium:

$$C_{O_2} = \%O_2 \cdot O_2^* = 20\% \cdot O_2^*$$

3. Oxygen volume transfer coefficient ($k_L a$)

Once all the parameters are calculated, equation (15) is applied.

$$k_L a_{O_2} = \frac{OUR}{(C_{O_2}^* - C_{O_2}) \cdot 1 \text{ mmol}/32 \text{ mg}}$$

APPENDIX VII

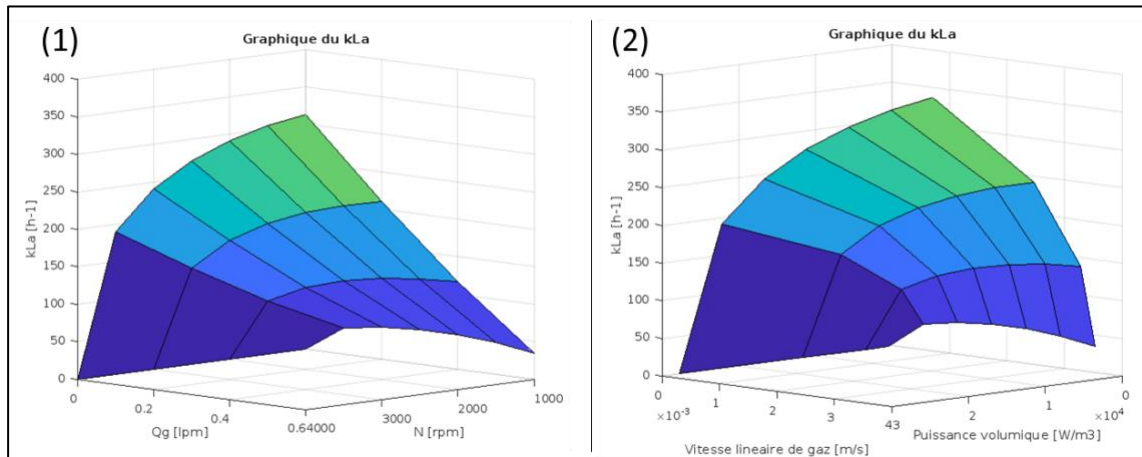
Response surface plots of the k_La - Matlab

Figure 2. Response surface of k_La - Ambr250.

(1) As a function of conditions. (2) As a function of the parameters (P/V and U_g).

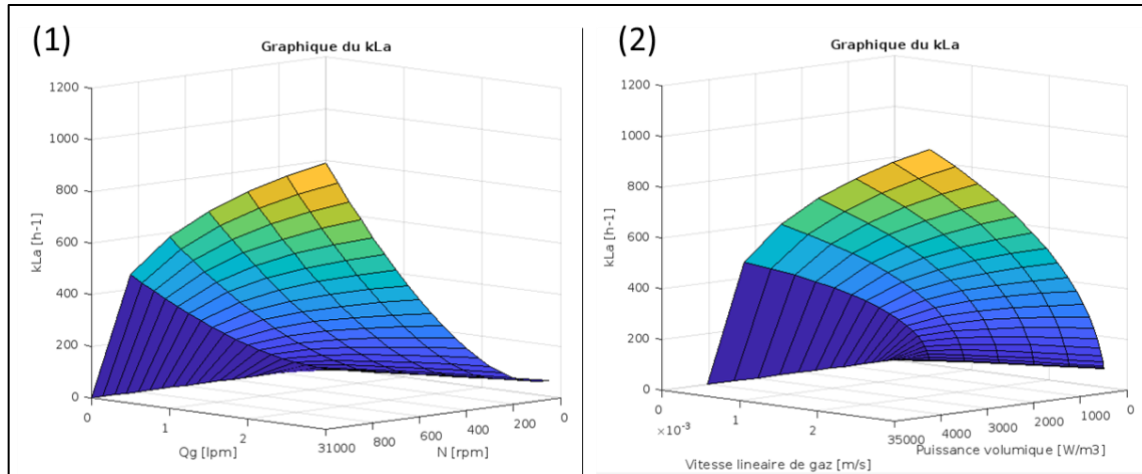


Figure 3. Response surface of the k_La - Biostat.

APPENDIX VIII

Reference scale data

Table 13. *MenB coli* process data in 1000 L and 5 L* bioreactors.

Bioreactor		1000L	5L
Middle Batch	V [L]	506	3,7
	Traces		
	[L]	5,7	0,032
	Inoculum		
	[L]	4,5	0,035
	T [°C]	37	37
	pH	6,8	6,8
	DO	100%	100%
	Qg Air	200	1.5 then 5
	[lpm]	then 500	lpm
Set point			
Regulation	pO ₂	20%	20%
		50 -	300 - 2000
	Agitation	259 rpm	rpm
	Air	-	-
		0 -	
	Oxygen	500 lpm	0 - 5 lpm
FB			
Middle Fedbatch	Medium [L]	190	2,2
	H ₃ PO ₄	2,5 N	2,5 N
	Antifoam	15%	15%

NH₄ OH

5N

85 L

0,5 L

IPTG

1,2 L

8 mL

**Data extracted from Sanofi's internal documents.*

Results of the reference scale (5L)

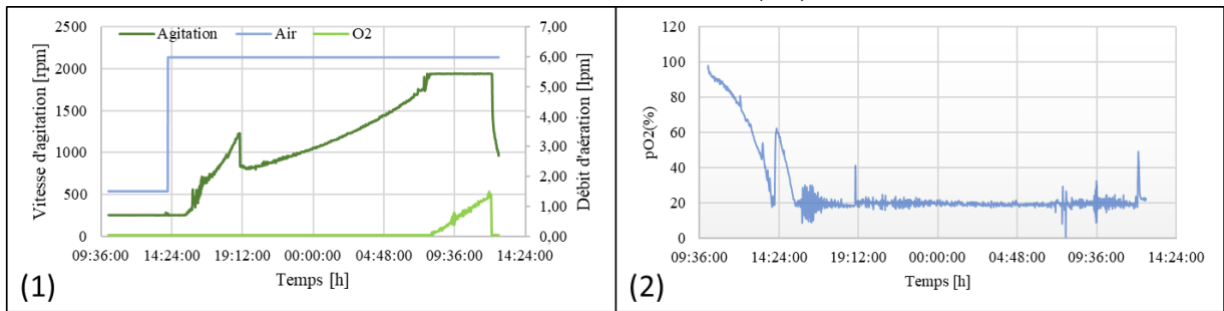


Figure 4. Profile of the 5 L bioreactor. (1) Operating conditions. (2) pO₂ regulation.

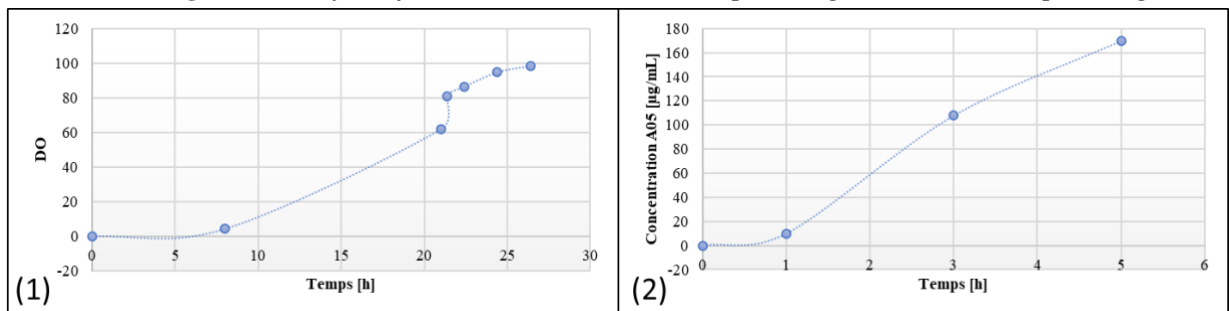


Figure 5. Results from the 5 L bioreactor. (1) Cell growth. (2) Antigen concentration.